SP2 Human Brain Organisation – Results for SGA2 Year 2 (D2.7.2 – SGA2)

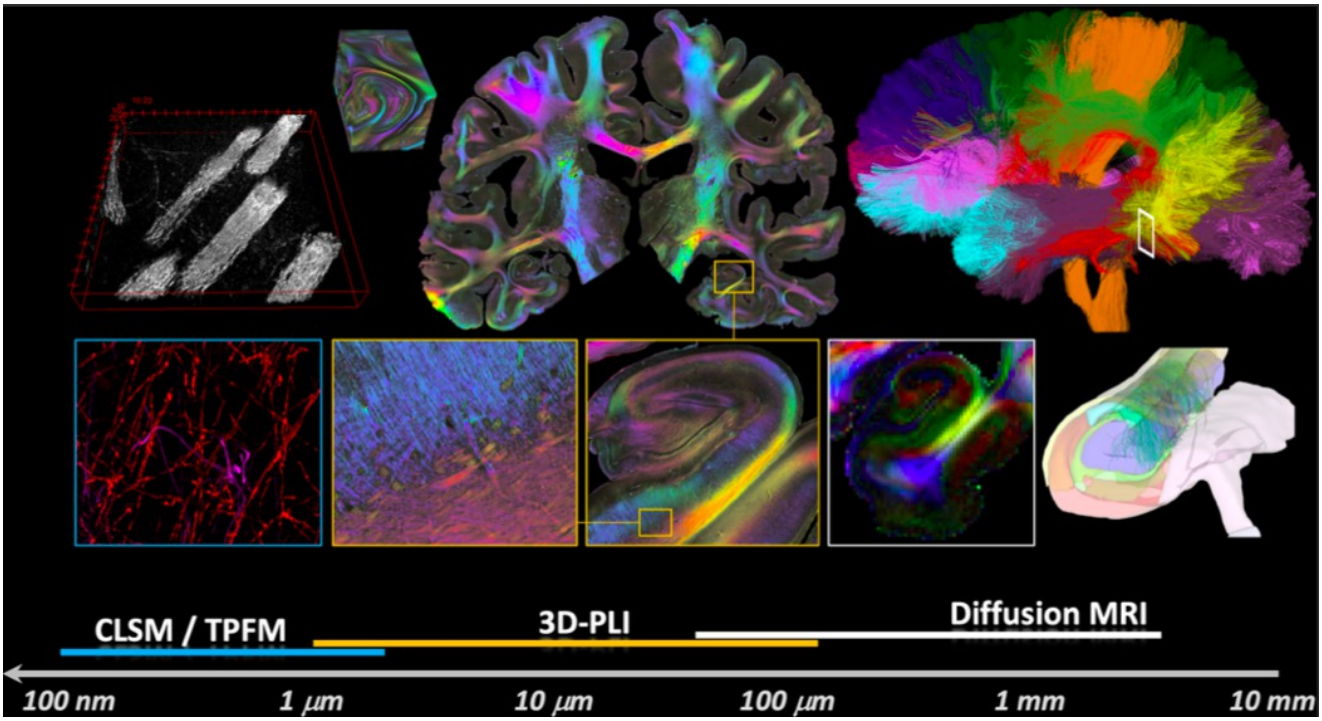

Figure 1: High-resolution fibre reconstruction at micrometer resolution.

Progress in "bridging the scales" has been achieved by applying multiple techniques to compute a high-resolution fibre reconstruction with unprecedented complexity of the human hippocampus. For the first time, three different modalities were combined: (i) high-field and strong gradient diffusion MRI (dMRI), (ii) 3D-Polarised Light Imaging (3D-PLI), and (iii) Two-Photon-Fluorescence Microscopy (TPFM). The same sample was imaged with PLI and Tractography and anchored to the BigBrain space / HBP human brain atlas.

Project Number:	785907	Project Title:	Human Brain Project SGA2

Document Title:	SP2 – Human Brain Organisation – Results for SGA2 Year 2
Document Filename:	D2.7.2 (D14.2 D36) SGA2 M24 ACCEPTED 201005.docx
Deliverable Number:	SGA2 D2.7.2 (D14.2, D36)
Deliverable Type:	Report
Work Packages:	WP2.1, WP2.2, WP2.3, WP2.4, WP2.5, WP2.6, WP2.7
Key Result(s):	KR2.1, KR2.2
Dissemination Level:	PU = Public
Planned Delivery Date:	SGA2 M24 / 31 Mar 2020
Actual Delivery Date:	SGA2 M26 / 27 May 2020; approved 30 Jul 2020; resubmitted 1 Oct 2020; accepted 5 Oct 2020
Author(s):	Katrin AMUNTS, JUELICH (P20) Jean-Francois MANGIN, CEA (P11) Francesco PAVONE, LENS (P40) Pieter ROELFSEMA, KNAW (P91) Francesca IANNILLI, JUELICH (P20)
Compiled by:	Francesca IANNILLI, JUELICH (P20)
Contributor(s):	Bertand THIRION (INRIA, P33) Jean-Philippe LACHAUX (UCL, P108) Timo DICKSCHEID, JUELICH (P20) Nicola PALOMERO-GALLAGHER, JUELICH (P20) Sarah GENON, JUELICH (P20) Simon EICKHOFF, JUELICH (P20) Sven CICHON, UNIBAS (P112) Svenja CASPERS, JUELICH (P20) Irene COSTANTINI, LENS (P40) Huib MANSVELDER, VU (P113) Wim VANDUFFEL, KUL (P111) Markus AXER, JUELICH (P20) Dirk FELDMEYER, JUELICH (P20) John ASHBURNER, UCL (P82) Anne van HAM, KNAW (P91) Claus HILGETAG, UKE (P75)
SciTechCoord Review:	N/A
Editorial Review:	N/A
Description in GA:	For consistent presentation of HBP results, SGA2 M24 Deliverables describing the accomplishments of an entire SP, WP or CDP have been prepared according to a standard template, which focuses on Key Results and the outputs that contribute to them. Project management elements such as Milestones and Risks will be covered, as per normal practice, in the SGA2 Project Periodic Report.
Abstract:	The main goal of SP2- human brain organisation- is to provide new insights into the multi-level organisation of the human brain, by bridging the different levels of its organisation in space and time, and deriving therefrom a rich set of neuroscientific

	data ranging from the molecular to cellular level up to local neural circuits and systems network levels, using state-of-the-art methods and techniques, and to share these data and new tools with the international science community through the HBP Human Brain Atlas.
Keywords:	Human Brain Atlas, Receptor densities, fibres, PLI, *fastpli*, JuGEx, connectivity matrix, neuron morphology and physiology, comparative studies, cognitive function
Target Users/Readers:	neuroscience community, clinicians, computer scientists, modelers, neuroimaging community

Table of Contents

Table of Tables

Table of Figures

History of Changes made to this Deliverable (post Submission)

Date	Change Requested / Change Made / Other Action
27 May 2020	Deliverable submitted to EC
30 Jul 2020	Deliverable approved by EC
1 Oct 2020	Minor editorial change by PCO
1 Oct 2020	Revised version resubmitted to EC by PCO via SyGMa

1. Overview

Subproject 2 (SP2) addresses human brain organisation at its multiple scales in space and time. We use and develop empirical methods to study the different levels of brain organization from the molecule to large-scale networks involved in cognitive functions. Having always in mind the organization of the brain as an organ, we have placed emphasis on the visuo-motor system, and the hippocampal region, where most comprehensive data sets have been acquired. A model of the multi-level organisation of visuo-motor integration has been developed, based on comparative fMRI studies in humans and monkeys.

SP2 has provided empirical findings on brain organization and shared its data with the research community via the HBP atlas – key part of Co-Design Project 3. In particular, we have contributed new maps of functional brain segregation, and its connectivity. The 3D probabilistic cytoarchitectonic atlas of the human brain includes 248 areas and nuclei, and has full cortical coverage; this data set serves as an interface to other modalities, and as a tool for modelers, e.g., such as those developed in Subproject 4, Theory.

SP2 provides new insights into the multi-scale connectivity of the brain, by measurements within one and the same tissue sample: a whole human hippocampus has been reconstructed by applying high-field (11.7T), strong gradient based anatomical and diffusion MRI, and 3D-Polarised Light Imaging. Two-Photon-Fluorescence Microscopy was also used to reveal the within-section fiber architecture on selected hippocampus sections (Fig.1).

This work will be continued in SGA3 in WP1, focusing on connectivity across the different scales, and WP3 that aims to develop new artificial networks based on such knowledge. WP4 continues to develop the Human Brain Atlas and WP6 is key to support, compute and storage intensive human brain research such as developed in our Subproject.

2. Introduction

The goal of Subproject 2 (SP2) is to provide new insights into human brain, approaching its multi-dimensional organisation. We addressed this aim by focusing our activities along the following Workpackages:

1) Multimodal whole brain mapping
2) Development of a cognitive architecture for visuo-motor integration tasks based on the multi-level organization of the human brain
3) Multi-modal, high resolution model of the human hippocampus including cells, fibres, receptors, gene expressions for theory, modelling, simulation and atlas
4) Inter-subject variability of the human brain at its relation to geno- and phenotype
5) Cross-species comparisons of mouse, rat, monkey and human brains in visuo-motor areas and medial temporal lobe
6) Develop and apply tools in co-design projects to bring the knowledge and the results to the scientific community

This work is carried out in close collaboration with the Neuroinformatics Platform (NIP, Subproject 5), mainly driven by Co-design project 3 (CDP3). Together we aim to develop new tools to make human brain data available and usable via the HBP Human Brain Atlas, which is the world's first and most comprehensive collection of curated multi-scale, multi-species, neuroscience data, along with viewers, analysis tools, a knowledge graph and tools for data import and export. As of today, no other repository offers a comparable set of cross-aligned labelled human brain data, and the possibility to adapt them to three standard spaces, including the unique microscopical BigBrain model. Another strong link with partners is established through CDP4, which aims to understand the mutual interactions between action and perception by combining neuroimaging (using tools such as fMRI), neurocomputational modelling, machine learning and robotics. Our collaboration lead to the development of an empirically derived visuo-motor integration neural network model focusing on visually guided eye movements and visually guided reach movements, running on the neurorobotics platform (Subproject 10). Moreover, the optical techniques and the software tools for the management of big data, developed in the frame of human brain samples analysis with light-sheet microscopy were also used in Subproject 1 and CDP1, for the reconstruction of whole mouse brain. Finally, the collaboration with CDP6 led to the development of mathematical models integrating the effect of cholinergic neurotransmission on activity levels in segregated brain regions, thus improving our understanding of the molecular features underlying drug-receptor interactions.

While all Workpackages (WPs 1, 2, 3, 4,5,6) finally contribute to the *Multi-modal and multi-scale human brain atlas* (Key Result 1 of Subproject 2 (KR 2.1)), some work on the hippocampus (WP3) contributes to a *high – resolution reconstruction of nerve fibre architecture applying 3 different imaging techniques in the same brain sample* (KR2.2.), which is targeted to a single region (as compared to whole brain) and has a strong methodological component.

Additional SP2 outputs can be found in CDP3 M24 compound Deliverable (D2.7.4) and CDP4 M24 compound Deliverable (D2.5.1).

3. Key Result KR2.1: Multi-model and multi-scale human brain atlas

The human brain is organized on multiple levels in space and time. While there are excellent resources worldwide in the field of neuroimaging (e.g, FSL, HCP), genetic data (Allen brain) or at the single cell level (neurodata.org), a link between data, i.e. scales and modalities has never been established in a comprehensive way, and research remained highly fragmented. We aimed to systematically bridge the different scales of organization, to link data between different species, and to develop an integrative atlas concept.

Several unique data sets have been created. E.g., IBC was extended and iEEG datasets were integrated in the Knowledge Graph. IBC is a unique asset providing a large variety of fMRI-based cognitive neuroscience experiments performed within one the same subjects (N=12) over many time points (up to 30 MRI sessions). The iEEG datasets stem from epileptic patients and provide the unique opportunity to access the human brain functioning with the temporal resolution of neuronal interactions. The cytoarchitectonic probabilistic maps includes now 248 areas and nuclei; this data set serves as an interface to other modalities. Furthermore, the multi-modal reconstruction of the hippocampus is enriched with receptorarchitectonic data. The structural connectivity dataset has now been implemented as connectivity matrices in the Atlas viewer. Also, we have established several brain-phenotype associations to characterize human brain variability, and integrated functional data on visual-motor transformations in the HBP Atlas. We have released a new version of a Python library for JuGEx (JuBrain Gene Expression analysis) and generated the first 3D high-resolution cytoarchitectonic maps in the BigBrain Atlas. Finally, we have optimised a prototype for semi-automatic interactive tool for mapping cytoarchitectonic areas across an unregistered series of consecutive histological sections and implemented an improved Convolutional Neural Network (CNN)-based sulcus recognition software. All these developments set the stage for an unprecedented level of data integration.

3.1 Overview of Outputs contributing to KR2.1

Below the list of SP2 outputs contributing to this KR, for more details see below.

Output number	Component	Name
1	C365	Individual Brain Charting dataset
2	C2245	Whole brain functional dynamics (iEEG recordings)
3	C2272, C2319	Cytoarchitectonic mapping
4	C2632	A common computational architecture for eye and arm movement control
5	C2287	Neuronal mechanism transforming a visual stimulus into an eye movement plan
6	C2634	Learning eye movement and grasping control using deep learning networks with brain-constrained architectures
7	C2306	Software for multimodal parcellation
8	C2315	Receptorarchitecture of the rat and human hippocampus
9	C2312, C2313	Brain-phenotype associations
10	C2314	The genetic basis of brain variability
11	C2362	Manifolds of the cortical patterns
12	C2317	Quantitative description of interneuronal distributions in primary and secondary visual cortex
13	C2351	Multi-modal characterization of human temporal neocortex

14	C2345	Functional characterization of cholinergic and adenosine modulators in motor and sensory cortices of rodent brains
15	C2318	Quantification of multiple receptor distributions in primate and rodent visual areas
16	C2470, C2322	Neuronal activity in the early visual system of mouse, monkey and human
17	n/a	New release of Phyton library for JuGEx (JuBrain Gene Expression analysis)
18	C2260	Connectivity matrix browser for the human brain atlas
19	n/a	Software library for microstructure detection and matching
20	C2271	Layer specific cell density in human visual areas
21	C2376	Optimised prototype for semi-automatic label propagation across cell-stained histological sections
22	C2356	Fibre analysis through large human brain areas
23	C2259	CNN-based sulcus recognition
24	C2259	Aligning great ape template spaces
25	C2577	Objective function for matching images to tissue probability maps
26	C2579	Patch-based Bayesian CCA methods
27	C3024	Enriching the Human Connectome

3.1.1 How Outputs relate to each other and the Key Result

A major goal of SP2 is to generate data on the structure and function of the human brain, tools to analyze the human brain data, and to provide new links to data from corresponding brain structures in experimental animals where these brain activity patterns can be studied with invasive techniques, hence providing higher-resolution data and information about the involvement of these brain structures in behavior.

Research in SP2 resulted in a number of unique datasets and tools, with important new crosslinks. E.g., information on the functional segregation of 12 subjects of the IBC project (output 1) was correlated to the iEEG recordings (output 2) to enable their joint analysis both at local and network level, which is synergistic as it reflects different aspects of brain dynamics for specific cognitive functions. Furthermore, the cytoarchitectonic maps (output 3) are used for the analysis of gene expressions (JuGEx, output 17).

In addition, cytoarchitectonic maps of human brain areas subserving visuo-motor integration tasks and functional dataset on visual motor-integration (output 5) are actively used for neural network models (e.g., models performing visuo motor integration tasks in outputs 4, 6 and CDP4, see D2.5.1) and for cross-species comparison studies (output 16).

Moreover, the connectivity-based parcellation of the hippocampus and the temporal lobe, which was obtained using the software for multimodal parcellation (CBP toolbox, output 7) is now integrated with neuronal distributions and morphology (outputs 6 KR2.2), fiber architecture reconstruction (outputs 1, 3, 4 KR2.2) and receptor architecture of different neurotransmitters and receptor types (outputs 8) to compute a multi-modal high-resolution reconstruction of the hippocampus.

Datasets in outputs 9, 10 and 11 disclose the inter-subject variability of the human brain in relation to genotype and phenotype. The structural connectivity datasets in output 9 have been anchored to the HBP Atlas (KR2.1) through the connectivity matrix browser (output 18). Furthermore, the genetic data in output 10 have been re-implemented in the HBP Atlas (KR2.1) as a python library (output 17). In addition, the datasets on cortical folding (output 11) have been used to build a new user-friendly sulcus-based alignment toolbox (output 23).

The new datasets on morphology, connectivity and distribution of inhibitory interneurons in different areas of the human brain are compared to similar data in monkeys and rodents (outputs 12, 13, 15). Functional insight into the role of those neurons are provided in outputs 14, 16.

The software (output 19) and the prototype (output 21) were exploited to compute the first precise 3D high-resolution maps of cortical layers and cytoarchitectonic areas in the human visual area (output 3), which, in turn, have been used to derive layer-specific cell density measures (output 20). Furthermore, the software tool for fiber analysis (output 22) has been used to estimate fiber orientation in TPFM- images (output 3, 4 from KR2.2). Outputs 23-26 are essential for the hyperalignment of all the datasets (outputs 1-16, except for 4, 6, 7) into the HBP atlas (KR 2.1); in particular, output 26 performs hyperalignment of diverse MRI datasets (output 1, 2). Finally, the on-line version of the historical von Economo & Koskinas atlas (output 27) contributes to the HBP Atlas by providing essential brain architecture data (KR2.1, output 20).

Thus, SP2 has achieved multiple important scientific goals and, in the process of doing so, has developed numerous data sets and tools that are highly beneficial to the neuroscience research community at large.

3.2 Outputs contributing to the multimodal whole brain mapping (WP2.1)

Research in this Workpackage results in maps (cytoarchitectonic, functional, connectivity), at different spatial scales. Note that output 7 from KR2.2 contributes also to this WP.

3.2.1 Output 1: Individual Brain Charting dataset

Dataset component: SGA1/SGA2 T2.1.1 Full human brain activity maps (volumes), ID: C365

Leader: Bertrand THIRION

The IBC dataset is a high spatial-resolution, multi-task, functional Magnetic Resonance Imaging dataset, intended to support the investigation on the functional principles governing human cognition. The concomitant data acquisition from the same 12 participants allows to obtain in the long run finer cognitive topographies, free from inter-subject and inter-site variability. The actual, second release provides more data from psychological domains. It includes tasks on e.g. mental-time travel, reward, theory-of-mind, pain, numerosity, self-reference effect, speech recognition, and video watching. In total, 20 tasks with >100 conditions were added to the dataset and >80 new cognitive components were included in the cognitive description of the ensuing contrasts.
The datasets are released and therefore curated (Table 1), and results have been published (see publication section); 3 other follow-up papers are in preparation.

Table 1: Output 1 Links

Component	Link to	URL
C0365	Data Repository	https://kg.ebrains.eu/search/instances/Dataset/8473a74b4dcb43d8a8bfda8326f75542 https://neurovault.org/collections/6618/
	Technical and User Documentation	https://project.inria.fr/IBC/data/

3.2.1.1 Actual and Potential Use of Output 1

The output is mostly designed for SGA3 activities, in two main work-packages:
SGA3/WP1: analysis of cognitive states in terms of topographies, state models and dynamics, where the IBC is integrated with other HBP datasets (iEEG, Diffusion-weighted MRI, fMRI-EEG) to provide adequate signatures of brain activity;
SGA3/WP2: System-level characterization of cognition based on brain activity correlates.

3.2.2 Output 2: Whole brain functional dynamics (iEEG recordings)

Dataset component: SGA2 - T2.1.2 Whole brain functional dynamics (iEEG recordings), ID: C2245

Leader: Jean-Philippe LACHAUX

We collect intracranial EEG data from participants in a set of cognitive tasks covering visual and auditory perception, memory, attention, language, and motor behavior. IEEG are the only recordings with both millimetric and millisecond precision that can be collected in the human brain. This spatio-temporal precision is required to reveal the fine neural dynamics supporting most of daily life cognitive processes, such as access to meaning, object identification. This output is a continuation of a consistent data collection initiated in the ramp-up phase, to increase the existing human intracranial database with 20 new patients, in a widespread international data format (BIDS). This **new dataset** has been uploaded to the HBP servers (curated, but under DPO review, Table 2). Data are provided with a novel navigation/visualization software, HiBoP (https://kg.ebrains.eu/search/?facet_type[0]=Software&q=HiBoP#Software/44532c17-f8c3-42b6-93ee-665726e792bc), specially designed for large iEEG datasets.

Table 2: Output 2 Links

Component	Link to	URL
C2245	Data Repository, Technical and User Documentation	https://kg.ebrains.eu/search/instances/Dataset/f3c976ed-1194-4990-9c2d-4c5007336284?group=public

3.2.2.1 Actual and Potential Use of Output 2

The number of potential users is difficult to estimate: without such data, it would simply be impossible to constrain neural models of human cognition, because all local and long-distance communication mechanisms that allow the cortex to work as a network, are based on fast neural activties (such as theta, alpha, beta oscillations, ranging between 4 and 40 Hz, high-frequency components in the gamma band above 40 Hz …, etc.) in very specific, task-dependent, brain regions. This dataset is also of interest for clinicians interested in the relationship between epilepsy and cognition.

3.2.3 Output 3: cytoarchitectonic maps of the human brain

Dataset component: SGA2 T2.1.4 Cytoarchitectonic maps, ID: 2319;

Dataset component: SGA2 T2.1.4 Cytoarchitectonic mappings in Big Brain visual areas, ID: 2272

Leader: Katrin AMUNTS

Cytoarchitectonic mapping of the human brain has resulted in new maps. A first version of a cortical map covering the complete cortex has been computed (manuscript under revision). Such full coverage is the basis for a comprehensive microstructural characterization of the brain, including both cortical areas and subcortical nuclei, while considering intersubject variability, interhemispheric and sex differences. This map represents a reference for modeling the human brain, both healthy subjects and patients, using, e.g., TVB. During the last year, areas of the lateral orbitofrontal cortex have been published (P2432), and a new map of the higher auditory cortex has been proposed (Zachlod et al., *Cortex*, 2020, *in press*). The latter shows a new hierarchical model of cytoarchitectonic segregation, which supplements existing models in non-human primates and functionally based parcellations. Probability maps of anterior cingulate areas provided novel insights into the role of this brain region in the processing of fear, sadness (P1328) and aggressive (P1375) behavior highlighting its crucial role in the regulation of emotion and aggression required for cognitive and social functioning. In addition, new opercular areas (PhD finished, DOI assigned) and

a new area in the anterior insula, related to logical negation (P2307) were mapped. Mapping in the prefrontal, orbitofrontal, temporal, occipital cortex as well as in some subcortical regions in progress; detailed analyses of the subgenual cinguate cortex, the posterior intraparietal cortex, the parieto-occipital cortex and the supplementary and presupplementary motor cortex have been published (P1629, P1392). Maps are provided in the single subject template of the MNI (colin27) as well as in asymmetric average template (MNI152), and we started to generate maps in the BigBrain space (see M12 D2.1.1 for component C2272, Table 3). Datasets are curated.

Table 3: Output 3 Links

Component	Link to	URL
C2272	Data Repository, Technical and User Documentation	https://kg.humanbrainproject.eu/instances/Project/af8d3519-9561-4060-8da9-2de1bb966a81
C2319	Data Repository, Technical and User Documentation	https://doi.org/10.25493%2F8EGG-ZAR

3.2.3.1 Actual and Potential Use of Output 3

Cytoarchitectonic maps are used for JuGEx (see output 17), a tool for differential analysis of gene expressions from the Allen Atlas according to regions defined in the JuBrain atlas; the tool is embedded as an interactive plugin into the HBP interactive atlas viewer.

The BigBrain has been developed into a commonly accepted standard reference. As a reference brain, it represents a unique template space of the HBP Human Brain Atlas.

3.3 Outputs contributing to the Development of a cognitive architecture for visuo-motor integration tasks based on the multi-level organization of the brain (WP2.2)

This Workpackage uses multi-level and multi-species brain data to assign and model computational functions for more than 20 human brain areas subserving visuo-motor integration tasks.

3.3.1 Output 4: A common computational architecture for eye and arm movement control

Model component: SGA2 T2.2.1 Visuo-motor integration model performing eye movement and reaching tasks, ID: 2632

Leader: Rainer GOEBEL

Our work mainly contributes to CDP4, by integrating neuroscientific knowledge, computational modelling, deep learning, experimentation and robotics to understand how the brain coordinates visually-guided actions. Researchers at UM, JUELICH, UPF and TUM are currently finalizing the integration of all functional modules (ganglion cell image resampling, object recognition, saliency computation, target selection & saccade generation) into an embodied large-scale cognitive architecture able to perform saccades for scene understanding. Models (curated) and respective URLs can be found in CDP4 deliverable D2.5.1.

3.3.1.1 Actual and Potential Use of Output 4

The extension of the NEST framework to include rate-based neuron models allows the implementation of functionally performant large-scale models. This let to biologically plausible spiking neuron models and functionally realistic rate neuron and mean field models within the same framework and hence facilitates gradual transitions between as well as integration of these (respectively bottom-up and top-down) modelling approaches.

3.3.2 Output 5: Neuronal mechanism transforming a visual stimulus into an eye movement plan

Dataset component: SGA2 - T2.2.2 Neuronal mechanism transforming a visual stimulus into an eye movement plan, ID: 2287

Leader: Pieter ROELFSEMA

The goal was to expand our knowledge of visuo-motor transformations that occur in the brain by studying the role of the Superior Colliculus (SC), as this multi-layer structure receives visual and cognitive input from the cortex and is connected to motor-output structures (more details in M12 deliverable D2.7.1). Dataset are curated but under embargo (Table 4).

Table 4: Output 5 Links

Component	Link to	URL
C2287	Data Repository, Technical and User Documentation	https://kg.ebrains.eu/search/instances/Dataset/f5a6cbf3-7d74-4210-b8f1-236a9b44ea19

3.3.2.1 Actual and Potential Use of Output 5

Our results provide unprecedented insight into the interactions between visual and motor related structures. Within HBP, they are useful for models of visuomotor integration within CDP4 (i.e., saccadic target selection models) and for cross-species comparisons and validations (output 19, T2.5.6; comparative mapping of visuo-motor cortex in monkey & human). Furthermore, (meta)data is shared via EBRAINS to make it accessible for other researchers.

3.3.3 Output 6: Learning eye movement and grasping control using deep learning networks with brain-constrained architectures

Model component: SGA2 T2.2.4 Brain-constrained deep learning modules for visuo-motor integration tasks, ID: 2634

Leader: Rainer GOEBEL

Researchers at UM have previously developed an algorithm which resamples images in accordance with ganglion cell distributions in the human retina. This resampling is incorporated as an initial step in convolutional neural networks to provide them with a human-like visual acuity drop-off with increasing distance from fixation. This forces these networks to explore a visual scene by taking snapshots from different fixations and integrate this information in order to recognise objects. Researchers at UM have also developed a biologically inspired recurrent neural network (RNN) for the control of finger joints of an anthropomorphic robotic hand.
Models (curated) and respective URLs can be found in CDP4 deliverable D2.5.1.

3.3.3.1 Actual and Potential Use of Output 6

The image sampling (blow-up) algorithm resamples images to reflect ganglion cell placement in the human retina and is relevant to increase the biological realism of models of the human retina. Efforts are currently ongoing together within SP4, notably Task T4.4.2 (Network model of the retina responding to complex stimuli; component id C2296). The biologically inspired recurrent neural network (RNN) constitutes a crucial first step towards achieving in-hand object manipulation using the same learning algorithm but a more sophisticated neural network architecture and is thus an important preparation for SGA3.

3.3.4 Output 7: Software for multimodal parcellation

Dataset component: SGA2 T2.2.1 Maps of the intraparietal sulcus on humans and non-human primates, ID: 2306

Component Leader: Simon EICKHOFF, Sarah GENON

We provide a python toolbox (https://github.com/inm7/cbptools, not curated yet) for the scientific community to conduct multimodal parcellations based on different MRI measures such as resting-state functional connectivity and probabilistic tractography (Reuter et al., *Brain Structure and Function*, 2020, P2431-*in validation process*; workflow in Fig. 2). The toolbox computes a connectivity matrix for each voxel in the region of interest with the whole brain's voxels. Voxels in the region of interest are clustered either in the same sub-region or different sub-region depending on the (dis)similarity of connectivity profiles. After clustering, validity criteria help to evaluate the obtained results in terms of how likely the parcellation pattern represent the ground truth. Dataset (C2306) produced with this tool are curated but under embargo (Table 5).

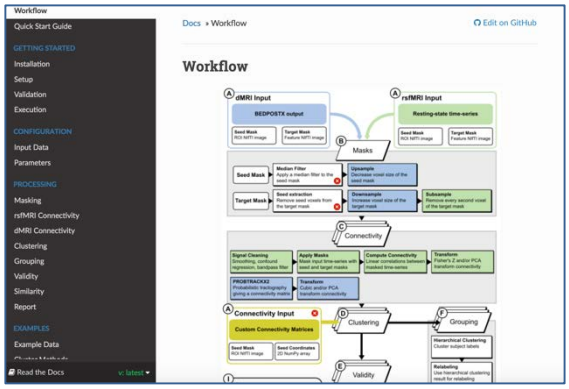

Figure 2: CBP software- workflow.

Table 5: Output 7 Links

Component	Link to	URL
C2306	Data Repository, Technical and User Documentation	https://kg.ebrains.eu/search/instances/Dataset/365d20da-0d22-43a5-9bf8-49e14ab6ac89

3.3.4.1 Actual and Potential Use of Output 7

The software can be used to parcellate and to create region specific maps or whole brain atlases based on large-scale connectivity of resting-state and probabilistic tractography.

3.4 Outputs contributing to Multi-modal, high-resolution model of the human hippocampus including cells, fibres, receptors, gene expressions for theory, modelling, simulation and atlas (WP2.3)

This Workpackage aims to obtain a description of the human hippocampal complex using various techniques that will produce different functional and morphological data of the region itself. Note that also outputs 1, 3, 4, 6 from KR2.2 belong to this WP.

3.4.1 Output 8: Receptorarchitecture of the human and rat hippocampus

Dataset component: SGA2 T2.3.5 Quantification of multiple receptor distributions for hippocampal regions and layers, ID: 2315

Leader: Nicola PALOMERO-GALLAGHER

Datasets provide densities of receptors for glutamate, GABA, acetylcholine, noradrenaline, serotonin and dopamine in the dentate gyrus, Cornu ammonis regions 1-3 and their layers of the rat and human hippocampus. We used the cytoarchitectonic maps provided by the HBP atlases for anatomic identification of hippocampal regions (Jubrain and Waxholm Space Rat Brain Atlas).

These results underlie the receptorarchitectonic maps included in the multi-modal model of the human hippocampus. They are unique, as they show the simultaneous quantification the densities of 15 different receptor types in the same tissue sample and enabling their comparison with other areas of the neural circuitry of cognitive emotion regulation, such as the amygdala. Datasets have been curated and released (Table 6).

Table 6: Output 8 Links

Component	Link to	URL
C2315	Data Repository, Technical and User documentation	Human: CA1: https://doi.org/10.25493%2FY7YV-6Q6 CA2: https://doi.org/10.25493%2F4F4S-W5A CA3: https://doi.org/10.25493%2FXFHR-X41 DG: https://doi.org/10.25493%2FM8PK-C82 CAcell: https://doi.org/10.25493%2F9DDZ-SJP CAmol: https://doi.org/10.25493%2FKYZ2-4GM rat: CA1: https://kg.ebrains.eu/search/instances/Dataset/f61c27af-d18e-4abc-9b02-96c09d49e542 CA2: https://kg.ebrains.eu/search/instances/Dataset/18a2c78a-a2e7-42dd-b468-3efdfaea1c54 CA3: https://kg.ebrains.eu/search/instances/Dataset/74385d61-058f-4288-8711-440fe4b90840 DG: https://kg.ebrains.eu/search/instances/Dataset/f3a71b29-9074-42e2-a3ac-425e6a2ff0e9 CAcell: https://kg.ebrains.eu/search/instances/Dataset/19cc79ac-fecd-4576-90e3-e7cabd42fe9f CAmol: https://kg.ebrains.eu/search/instances/Dataset/904d8506-60ac-4dc6-85fd-83555bd2c5e4

3.4.1.1 Actual and Potential Use of Output 8

The results are part of the data implemented in two of the HBP atlases: the JuBrain Atlas, and the Waxholm Space Rat Brain Atlas. The datasets provide information concerning the molecular basis of modulatory neurotransmission in the dentate gyrus and CA1-CA3 regions in both species. Thus, they provide crucial constraints necessary to refine realistic whole brain models of neuronal networks.

3.5 Outputs addressing Inter-subject variability of the human brain at its relation to geno- and phenotype (WP2.4)

This Workpackage provides the neurobiological backbone as well as relevant exemplary markers for the quantification of inter-individual variability based on HPC analyses of large cohorts.

3.5.1 Output 9: Brain-phenotype associations

Software component: SGA2 T2.4.2 Structure-phenotype associations for JuBrain Atlas regions, ID: 2312

Dataset component: SGA2 T2.4.2 Association between brain structural features and phenotypes, ID: 2313

Leader: Svenja CASPERS, Simon EICKHOFF

We showed that combined lifestyle risk is associated with cortical atrophy in lateral prefrontal and premotor cortex as well as increased functional connectivity of these to other brain regions (P1666; Fig. 3). Moreover, we proved aging trajectories to be similar between cohorts, but with different effects of influences (e.g. age, gender, education or physical/ mental well-being), hinting at exercising caution when pooling different datasets (P1644). Additionally, specific phenotypes can be predicted from brain features, e.g. gender based on resting-state functional connectivity (P2034). We integrated information on structural connectivity matrices for all JuBrain Atlas regions.

We also aimed to provide a tool to characterize the behavioral profile of brain regions by relating interindividual variability in local grey matter volume and cortical thickness and psychometric data (P1777), and demonstrate that correlations and replicability rates for correlations between grey matter volume in dorsal premotor cortex and psychometric data were low. We are now developing a connectivity-based psychometric prediction framework to explore the relationships between interindividual variability in connectivity and behavioral phenotypes (CBPP, curated – Fig. 4; more details in D2.4.1):
https://kg.ebrains.eu/search/?facet_type[0]=Software&q=CBPP#Software/6489bce3-dfd5-406d-84f3-310d08f74af0 ;
https://github.com/inm7/cbpp/blob/master/README.md .

Datasets are curated but under DPO review (Table 7).

Table 7: Output 9 Links

Component	Link to	URL
C2312	Software Repository	https://github.com/shahrzadkh/pyJUSBB
	Technical Documentation	https://github.com/shahrzadkh/pyJUSBB/blob/master/README.md
	User Documentation	https://github.com/shahrzadkh/pyJUSBB/wiki
C2313	Data Repository, Technical and User Documentation	https://kg.ebrains.eu/search/instances/Dataset/e428cb6b-0110-4205-94ac-533ca5de6bb5

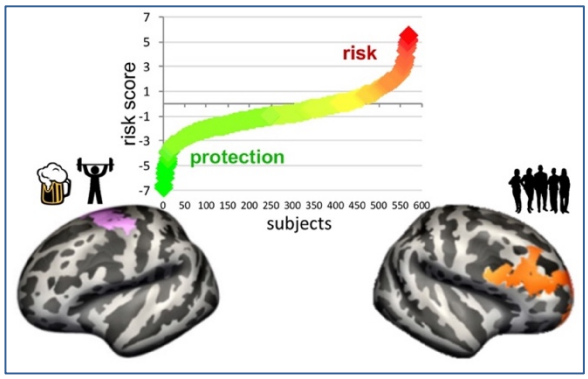

Figure 3: Combined lifestyle risk and its association with brain structure.

Atrophy in depicted brain regions mainly driven by factors visualized next to the regions.

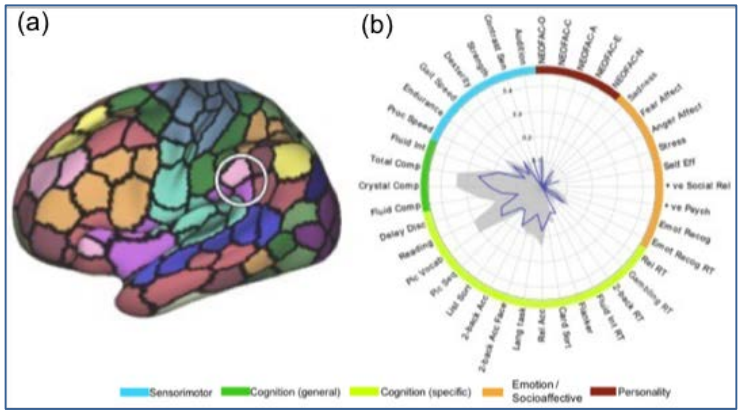

Figure 4: Parcel-wise connectivity-based psychometric prediction framework (CBPP).

Psychometric profiles for the pair of parcels in (a) Supramarginal gyrus (b) Broca region in left and right hemispheres respectively. Grey filled contour shows whole-brain prediction profile, while blue contour shows parcel-wise prediction profile.

3.5.2 Output 10: The genetic basis of brain variability

Dataset component: SGA2 T2.4.3 Contribution of genetics and functional connectivity on structural covariance, ID: 2314

Leader: Simon EICKHOFF, Sven CICHON

We assessed macroscale cortical axes based on structural covariance of thickness using advanced machine learning. We utilized a twin methodology to identify genetic influences on macro-scale organization in humans and compared humans and macaques, to understand the evolutionary basis of macro scale organization of thickness. Structural covariance of thickness was organized along anterior-to-posterior and inferior-to-superior axes (Fig. 5). We observed a strong correspondence between the large-scale organization of thickness covariance and genetic correlation of thickness. In addition, we observed similar organizational principles in macaque thickness covariance, providing evidence that macro scale organization of thickness is evolutionary conserved (Fig. 6). Dataset are curated, but under embargo (Table 8).

Table 8: Output 10 Links

Component	Link to	URL
Component 2314	Data Repository, Technical and User Documentation	https://kg.ebrains.eu/search/instances/Dataset/8620b6c0-3037-416d-a410-c77551ece50e

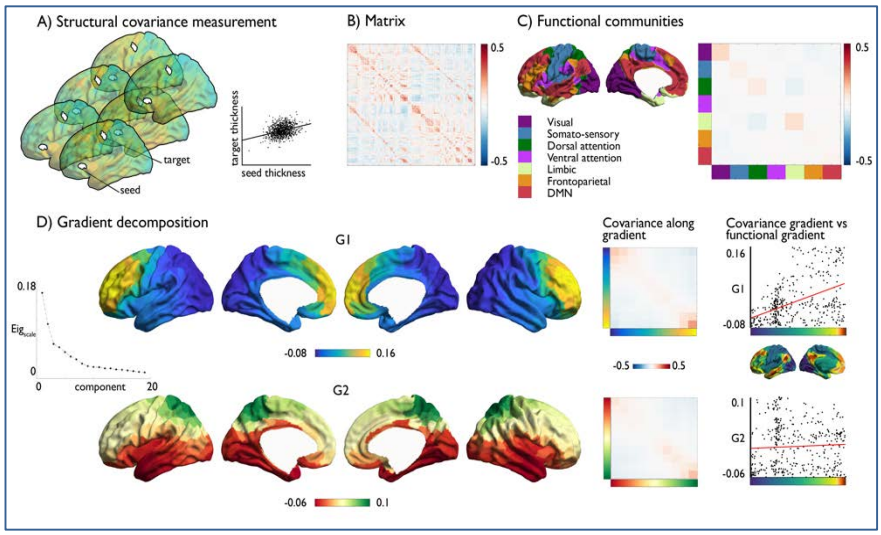

Figure 5: Structural covariance gradient in macaque monkeys.

A) Measuring structural covariance of thickness; B) Structural covariance matrix; C) mean correlation within functional network community; D) Gradient decomposition: primary gradient (G1) and secondary gradient (G2).

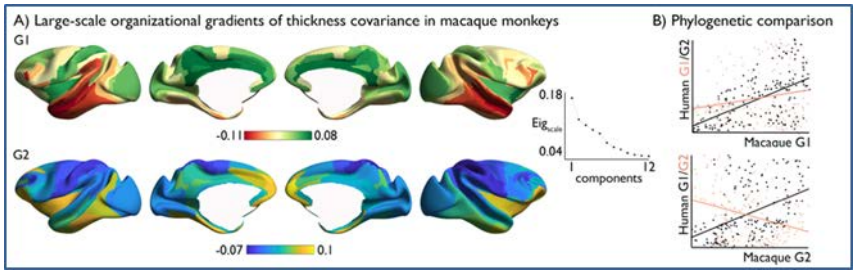

Figure 6: Large scale organization of structural covariance.

A) Measuring structural covariance of thickness. Gradient decomposition, primary (G1) and secondary (G2) macroscale gradient: red indicated a higher gradient ranking in humans, whereas blue indicates a higher gradient ranking in macaques; B) scatter plots indicate the association between human posterior-anterior covariance gradient (G1, black) and human inferior-superior covariance (G2, red) and macaque principal gradient (G1, upper scatterplot) and secondary gradient (G2, lower scatterplot).

In another study, we used a genetic risk score (GRS) based on twenty loci previously identified to be associated with late-onset Alzheimer's disease (AD), at genome-wide significance and evaluated the polygenic effects on cortical thickness of older adults from a population cohort (1000BRAINS). The presented data (curated) reflect the allelic scoring information to calculate six pathway-specific GRS and can be found at: https://kg.ebrains.eu/search/instances/Dataset/c404e7f6-9a18-4a5c-ae3c-27f159f4f96a .

3.5.2.1 Actual and Potential Use of Outputs 9, 10

The datasets are anchored to the HBP Atlas as connectivity matrices, therefore providing characterization of variability of the HBP Atlas regions.

3.5.3 Output 11: Manifolds of the cortical folding patterns

Dataset component: SGA2 T2.4.1 Dictionary of cortical folding patterns, ID: 2362

Leader: Jean-Francois MANGIN

We have further studied representations of the variability of the cortical folding pattern using manifold learning. For the adult human brains, the manifolds are computed from the 1000 subjects of the HCP dataset. In addition to using these manifolds to study the variability of the functional maps (more details in M12 deliverable D2.7.1), we have used them to study the variability of the shape and trajectories of the fiber bundles of the HBP atlas. We have completed our representations

with 1) studies of the onset of the folding variability using a longitudinal dataset of highly preterm infants, 2) cross species comparison in primates (Fig. 7; see also: Fouber O., et al. Comparison of the motor-hand area morphology in Great Apes, OHBM, Montreal, 2020, *submitted* and Mangin et al., *Brain Topography*, 2019, P2198-*in validation process*). Datasets are curated but under embargo (Table 9).

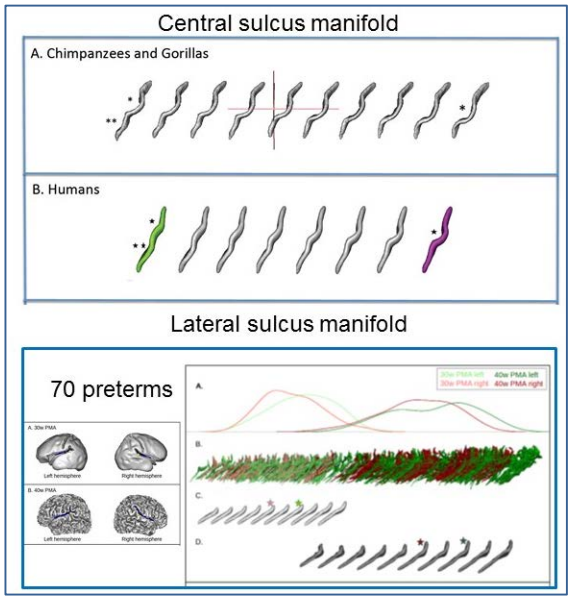

Figure 7: Cross-species comparison of cortical folding.

Top: Comparison of primates; Bottom: Developmental and across hemisphere variability in preterm infants.

Table 9: Output 11 Links

Component	Link to	URL
Component 2362	Data Repository, Technical and User Documentation	https://kg.ebrains.eu/search/instances/Dataset/3117192d-974f-4d8c-8a16-d33ef461ac92

3.5.3.1 Actual and Potential Use of Output 11

The new representations of the variability of cortical morphology have led to a new brain mapping framework imposing folding pattern compatibility before group analysis. This innovative strategy provides new understanding of the variability of functional maps and connectivity. It is also exploited to detect abnormal folding patterns signing abnormal developmental events, with ongoing projects on high prematurity (collaboration with Utrecht hospital) and Autism (collaboration with EU-Aims consortium). The design of a user-friendly toolbox to exploit this methodology is in progress, building upon the sulcus-based alignment toolbox of HBP (T2.6.3, Output 23).

3.6 Outputs in the context of Cross-species comparisons of mouse, rat, monkey and human brains in visuo-motor areas and medial temporal lobe (WP2.5)

Here we identify functional and structural features of the brain by analyzing inter-species differences and commonalities in mouse, rat, monkey and human brains in visuo-motor areas and the medial temporal lobe at different spatio-temporal scales.

3.6.1 Output 12: Quantitative description of interneuronal distributions in primary and secondary visual areas

Dataset component: SGA2 T2.5.3 Analysis of calcium-binding protein interneurons in human primary visual cortex and early extrastriate visual areas, ID:2317

Leader: Karl ZILLES, Roxana KOOIJMANS

We deliver scans of full (hemisphere) sections of human brain from the occipital pole to the splenium of the corpus callosum. The final scope of this task is to generate a quantitate description of interneuronal distributions in primary and secondary visual areas, as well as other extra striate visual regions. This achievement is based on the development of a novel staining protocol that allows the visualization of specific cell populations expressing calcium binding proteins parvalbumin, calbindin and calretinin in full size human brain sections. We acquire high-surface (full section), high-resolution (1um) scans of the processed tissue, and segment stained cell bodies using machine-learning and super-computing. Ultimately, we calculate the distributions of different cell populations, along the cortical depth, for the entire cortex (Fig. 8). Datasets are curated, but under embargo (Table 10).

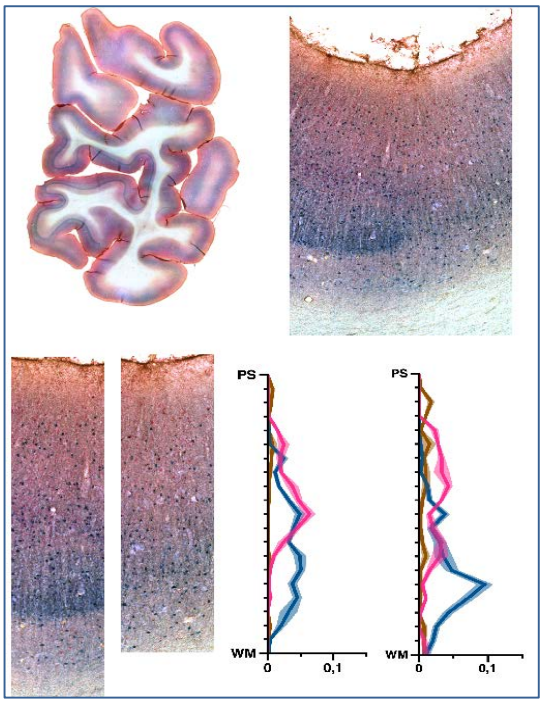

Figure 8: Full human section stained for calcium binding proteins.

The image shows human sections stained with parvalbumin (PV-blue), calbindin (CB-magenta) and calretinin (CR-brown), with detail of the area 17 (V1) to area 18 (V2) border, and cell density distribution profiles of respective samples.

Table 10: Output 12 Links

Component	Link to	URL
Component 2317	Data Repository, Technical and User Documentation	https://doi.org/10.25493%2F15ZS-BQB; https://kg.ebrains.eu/search/?facet_type[0]=Dataset&q=kooijmans#Dataset/73583e72-67f3-4e93-8f99-9ebefac14abe; https://doi.org/10.25493%2FC5KW-DMH

3.6.1.1 Actual and Potential Use of Output 12

The raw (scans) as well as derived (segmented cell bodies & calculated cell densities) data sets will be included in the atlas of the human brain project (KR2.1). The quantification, integrated in Tasks 1.1 and 1.3 of WP1 of SGA3 will be further refined and made compatible for The Virtual Brain.

3.6.2 Output 13: Multi-modal characterization of human temporal neocortex

Dataset components: SGA2 T2.5.2 molecular characterization of the interneurons in human temporal neocortex, ID: 2351

Leader: Francesco PAVONE, Irene COSTANTINI

Physiological recording from Somatostatinergic (SST), Vasointestinal peptide (VIP), and Parvalbuminergic (PV) interneurons were performed in two slices of human temporal neocortex from the same subject. On the same tissue a morphological analysis was performed. The slices were cleared with the SWITCH/TDE clearing protocol (details in M12 deliverable D2.7.1) and the same interneurons (SST,VIP,PV) were labelled using a triple staining method. Finally, a mesoscopic reconstruction of the entire slices in 3D were obtained using a custom-made two-photon fluorescence microscope, characterized by a resolution of 0.44 x 0.44 x 2 µm3 (Fig. 9). The combination of functional and structural information obtained from specific cellular sub-type in large 3D volume of human brain cortex of the same subject allows to bridge the gap between different modalities, providing a new multi-modal more complete view of the tissue.

Dataset are curated but under embargo (Table 11).

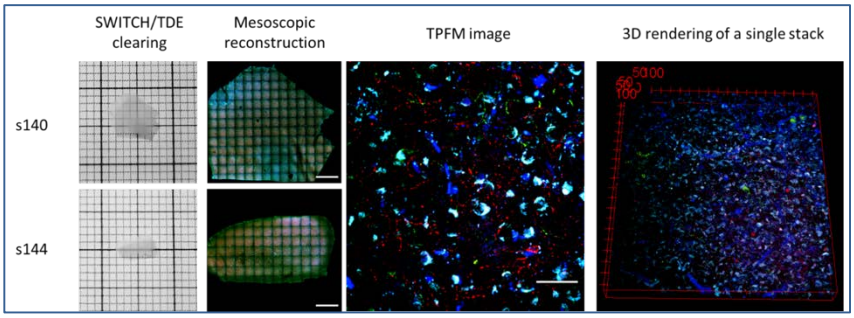

Figure 9: morphological analysis of human temporal neocortex.

Table 11: Output 13 Links

Component	Link to	URL
C2351	Data Repository, Technical and User Documentation	https://kg.ebrains.eu/search/instances/Dataset/27ad5531-9c67-4745-a22a-e40fea14f328

3.6.2.1 Actual and Potential Use of Outputs 13

Data have been shared with collaborators within HBP (SP1) and will serve as input for modelling and simulation (SP4, SP6).

3.6.3 Output 14: Functional characterization of cholinergic and adenosine modulators in motor and sensory cortices of rodent brains

Dataset component: Quantitative analysis of neuromodular function in the rodent neocortex, ID: 2345

Leader: Dirk FELDMEYER

We investigated a differential cholinergic neuromodulation of the excitability and synaptic activity in corticothalamic- and corticocortically-projecting layer 6 (L6) pyramidal cells (more details in M12 deliverable D2.7.1). We also characterized corticothalamically projecting FoxP2-positive pyramidal neurons in L6A and L6B of somatosensory cortex and their modulation by ACh and dopamine. These

data are entirely novel and add to the description of the neuron complement in the neocortex thereby contributing to KR2.1. Finally, we investigated the adenosine effects on L6 pyramidal neurons activity in prefrontal and somatosensory cortex and found that prefrontal pyramidal cells were much more susceptible to adenosine modulation than those in somatosensory cortex. This new data set contributes also to KR2.1. Datasets are curated (Table 12).

Table 12: Output 14 Links

Component	Link to	URL
C2345	Data Repository, Technical and User Documentation	Morphological data https://doi.org/10.25493%2FYMV3-45H ElectroPhysiological data https://doi.org/10.25493%2F93YQ-6QM Immunofluorescence data https://doi.org/10.25493%2FA4RG-CJN

3.6.3.1 Actual and Potential Use of Output 14

Data on cholinergic modulation of excitatory neurons are used by Markus Diesmann (SP4) to simulate the effects of acetylcholine on the neuronal network in the neocortex later to use the data on a project modelling cholinergic modulation in SP6. Also, these datasets are currently used by Henry Markram (SP4) for modeling of synaptic transmission and neuromodulation simulations of neocortical tissue. Outside HBP, our datasets are being used by Marcel Oberländer (at 'Ceasar', Bonn Germany) on constructing a model of a cortical interneuron column.

3.6.4 Output 15: Quantification of multiple receptor distributions in primate and rodent visual areas

Dataset component: SGA2 T2.5.4 Quantification of multiple receptor distributions in primate and rodent visual areas, ID: 2318

Leader: Nicola PALOMERO-GALLAGHER

Datasets providing the densities of different receptors for acetylcholine, noradrenaline, serotonin and dopamine in areas of the human, macaque monkey and rat visual cortices. Data is provided for areas V2d, V2v V3d and V3v of the human brain, for areas V1, V2d, V2v, V3d and V3v of the macaque monkey brain, and for areas Oc1M, Oc1B, Oc2M and Oc2L of the rat brain.

We used the cytoarchitectonic maps areas hOc2, hOc3d and hOc3v of the JuBrain atlas for identification areas in the human brain. The parcellation scheme arising from the analysis of visual areas in the rat brain will contribute to refine the map of the rodent neocortex which is made available via the Waxholm Space Rat Brain Atlas.

Datasets are curated (Table 13).

Table 13: Output 15 Links

Component	Link to	URL
C2318	Data Repository, Technical and User Documentation	human: hOc2d: https://doi.org/10.25493%2FZJ7E-KXZ hOc2v: https://doi.org/10.25493%2F2E5C-PVM hOc3d: https://doi.org/10.25493%2F4ETW-9XB hOc3v: https://doi.org/10.25493%2FTBMX-BZ9 monkey: V1: https://kg.ebrains.eu/search/instances/Dataset/8aadfc22-eb39-47af-b57d-e712570d6645 V2d: https://kg.ebrains.eu/search/instances/Dataset/e98e711f-6bd1-4743-b715-e58f98f601d9 V2v: https://kg.ebrains.eu/search/instances/Dataset/412ac691-fd3f-4f59-af5a-ba11afc5eb9f

		V3d: https://kg.ebrains.eu/search/instances/Dataset/ec2cdc31-ae42-4074-970c-1c0b455e90fd V3v: https://kg.ebrains.eu/search/instances/Dataset/1856dfa0-5708-41e1-8792-0559e166c903 rat: Oc1B: https://kg.ebrains.eu/search/instances/Dataset/b2c4e380-ce96-4325-8a82-f24c0143448b Oc1M: https://kg.ebrains.eu/search/instances/Dataset/a9a60163-a070-4611-896c-393b1d8342d9 Oc2L: https://kg.ebrains.eu/search/instances/Dataset/4a96960d-76f9-4c83-b1f6-4dc54be77a6e Oc2M: https://kg.ebrains.eu/search/instances/Dataset/ae50e708-0552-43b7-8bcd-aa3a002c687d

3.6.4.1 Actual and Potential Use of Output 15

Human data will be included in the HBP Atlas (KR2.1). Data from all three species can be included in the model of the multilevel organisation of visuo-motor integration tasks being developed in SP2 (KRc4.1, see deliverable D2.5.1). Results are unique, as they show the simultaneous quantification of the densities of multiple receptor types for different neurotransmitters in the same tissue sample.

3.6.5 Output 16: Neural activity in the early visual system of mouse, monkey and human

Report Component: SGA2 T2.5.6 Comparative mapping of visuo-motor cortex in monkey and human, ID: 2470

Dataset Component: SGA2 T2.5.6 Comparative mapping of visuo-motor cortex in mouse, monkey and human, ID: 2322

Leader: Wim VANDUFFEL, Pieter ROELFSEMA

The report component has been already described in deliverable D2.7.1.

We developed novel analytical tools to compare in an unbiased manner the cortical representation of multi-modal (visual, tactile and auditory domain) stimuli in human and non-human primates. E.g., we show that the fMRI signals measured in the monkey brain are better predictors (compared to predictors based on the stimuli themselves) for activity in the human brain in most of visual and somatosensory cortex, but not for auditory cortex (Fig. 10). Datasets are curated but under embargo (Table 14).

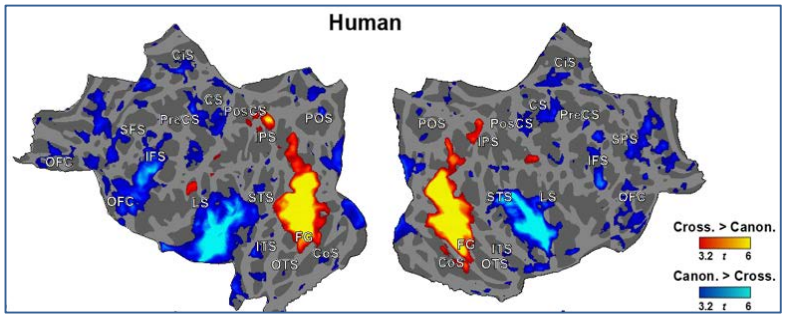

Figure 10: Performance comparison between cross-species and canonical models in humans.

We contrasted prediction performances between a cross-species model (whereby the recorded fMRI signal from one species, i.e., rhesus monkey, is used to analyze that of the other species, i.e. human) and the canonical model (based on the stimulation paradigm used, as in a regular GLM) in the human. We show difference maps thresholded at q < 0.05, FDR corrected. Maps show areas where the cross-species model performed better than the canonical model (in red) and vice versa (in blue). Outlines indicate the border of the visual (purple), auditory (green) and tactile (white) activation maps thresholded at q < 10-7, FDR correction.

Table 14: Output 16 Links

Component	Link to	URL
C2322	Data Repository, Technical and User Documentation	https://kg.ebrains.eu/search/instances/Dataset/9d8bf88b-d43d-4cbf-8d04-d43f9fda72c9 https://kg.ebrains.eu/search/instances/Dataset/088a7717-76d2-4520-b9e8-3f2fecce1ee4

3.6.5.1 Actual and Potential Use of Output 16

The group of Sacha VAN ALBADA (Brain Simulation Platform, SP6) is already implementing the neuronal data acquired here, in their canonical models of cortex.

3.7 Outputs contributing to Develop and apply tools in co-design projects to bring the knowledge and the results to the scientific community (WP2.6)

This Workpackage aggregates all the methodological efforts of the SP2's team to finalise tools that are either required as plugin in the HBP's digital infrastructures (mainly SP5), or required for high-throughput analysis of the data delivered by the other WPs of SP2. Note that outputs 2, 5 from KR2.2. also contribute to this WP.

3.7.1 Output 17: New release of Python library for JuGEx (JuBrain Gene Expression analysis)

Component: N/A

Leader: Timo DICKSCHEID

The original JuGEx algorithm for differential analysis of gene expressions by atlas regions1 has been reimplemented as a python library (Table 15), with a streamlined library design and better efficiency and stability. This library can be used for batch computations, and is the basis for a web backend serving the JuGEx atlas viewer plugin, which has been co-developed with T5.4.3. While the atlas viewer plugin provides a simple yet intuitive graphical user interface to run JuGEx experiments from the browser, the exact same computation can be executed in a Jupyter notebook using the python library. In fact, the viewer plugin can generate the python code for an experiment on request and open it in a Jupyter notebook in the collaboratory, allowing users to transition seamlessly from exploratory, more visually guided analysis, into sustainable and larger scale data experiments. Software is not curated.

Table 15: Output 17 Links

Component	Link to	URL
n/a[2]	Software Repository	https://github.com/FZJ-INM1-BDA/PyJuGEx
	Technical Documentation	https://github.com/FZJ-INM1-BDA/PyJuGEx
	User Documentation	http://www.fz-juelich.de/inm/inm-1/DE/Forschung/_docs/JuGex/JuGex_node.html

[1] Sebastian Bludau, Thomas W. Mühleisen, Simon B. Eickhoff, Michael J. Hawrylycz, Sven Cichon, Katrin Amunts. Integration of transcriptomic and cytoarchitectonic data implicates a role for MAOA and TAC1 in the limbic-cortical network. 2018, Brain Structure and Function. https://doi.org/10.1007/s00429-018-1620-6

2 This particular work has not been separately defined as a component in the workplan.

3.7.2 Output 18: Connectivity matrix browser for the human brain atlas

Software component: SGA2 T2.6.1 A Connectivity matrix export tool of the human atlas, ID: 2260

Leader: Timo DICKSCHEID

Together with T5.4.3, we co-developed new functionality in the interactive atlas viewer to select, browse and download connectivity matrices compatible with a given parcellation (C2260, Table 16). This includes connectivity data extracted from the 1000 brains cohort,[3] grouped by regions of the JuBrain cytoarchitectonic atlas. We are now working with the human data curation team (T5.3.1) to include new connectivity sources, e.g. the ARCHI database (https://kg.ebrains.eu/search/instances/Project/38535464-ec76-4d3e-8490-947c7778fe15), as well as in cooperation with T5.4.2 external cohort data like the UK Biobank. During this process, we contribute to the preparation and standardization of connectivity data, and to the design of atlas ontologies and the spatial metadata scheme SANDS carried out by WPs 5.1 and 5.3 (cf. KR5.4).

Table 16: Output 18 Links

Component	Link to	URL
C2260	Online service	https://atlases.ebrains.eu/viewer/
	Technical and User Documentation	https://interactive-viewer-user-documentation.apps-dev.hbp.eu/

3.7.2.1 Actual and Potential Use of Outputs 17, 18

The work in these outputs is directly concerned with the co-design of infrastructure components in SP5, to bring in the scientific expertise, datasets, methodology and coordination of the research on human brain architecture in SP2 into the development of tools and functionalities for the human brain atlas. Therefore almost all efforts in task 2.6.1 result in shared components with Tasks 5.4.3 and 5.3.3. Use and exploitation of this work is via users of the brain atlas services, as reported for KRs 5.1, 5.4, 5.6 and 5.7.

3.7.3 Output 19: Software library for microstructure detection and matching

Component: N/A

Leader: Timo DICKSCHEID

We further developed and improved the methodology for detecting cell bodies and vessels in microscopic scans of histological sections. The framework (not curated, Table 17) is now able to perform detections with classical image processing methods like thresholding and Watershed segmentation, traditional learning-based methods like AdaBoost, as well as trained CNN classifiers like U-Nets represented by TensorFlow models. We are performing an extensive evaluation of the performance of different classifiers in challenging settings with significant object overlaps and staining variations. We computed the first precise 3D reconstruction of local regions of interest at a precision level of single cells (Huysegoms et al., OHBM 2019, E1543). These have been used to extract cell densities (Output 20).

[3] https://www.fz-juelich.de/inm/inm-1/EN/Forschung/1000_Gehirne_Studie/1000_Gehirne_Studie_node.html

Table 17: Output 19 Links

Component	Link to	URL
n/a	Software Repository, Technical and User Documentation	https://github.com/FZJ-INM1-BDA/demics https://github.com/FZJ-INM1-BDA/colamatch

3.7.4 Output 20: Layer specific cell densities in human visual areas

Report component: Service for computing a map of cortical depth from a cortical segmentation, ID: 2271

Leader: Timo DICKSCHEID

The BigBrain model is composed from ~7400 cell-body stained histological sections, so its gray values can be interpreted as optical densities. The first 3D maps of cortical layers and cytoarchitectonic areas (cf. output 21, C2376) now make it possible to extract optical densities in cortical layers of several visual areas of BigBrain. Furthermore, the approach for cellular level 3D reconstruction mentioned in Output 19 (Huysegoms et al., OHBM 2019, E1543) allows to estimate layer-wise cell density from individual detections of cell bodies in small local regions of interest (Fig. 11). We created a first table of such layer-specific cell density estimates in visual areas, along with the numbers reported by von Economo4, showing high similarity of estimates particularly in layers II, IV and VI.

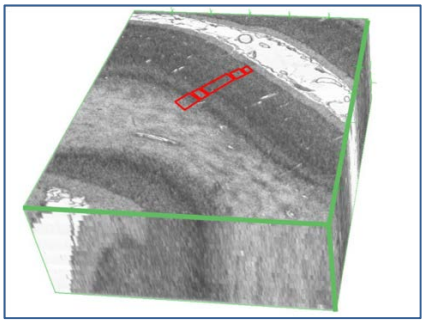

Figure 11: 3D reconstruction of a local region of interest in the visual cortex.

The 3D reconstruction is obtained at a precision level of individual cells, with manual delineation of patches in different cortical layers.

Table 18: Output 20 Links

Component	Link to	URL
C2271	Report and User Documentation	https://wiki.humanbrainproject.eu/bin/view/Collabs/cell-densities-bigbrain/

3.7.4.1 Actual and Potential Use of Outputs 19, 20

The software for microstructure detection is so far used by researchers in JUELICH to compute 3D reconstructions of local regions of interest from histological sections. It has been successfully applied to cell body stains as well as to immunohistochemistry stains for calcium bindings (Kooijmans et al., SfN 2019, E1544, E1545). As our methods for cellular level 3D reconstruction and precise cell detection mature, extraction of cell density measures in the BigBrain brings an enormous potential

[4] Economo, C., and Koskinas, G. N. (1925). "Die Cytoarchitektonik der Hirnrinde des erwachsenen Menschen." Springer-Verlag, Berlin.

not only for studying whole brain cytoarchitecture at high detail, but also for informing multiscale simulations. Therefore, Output 20 is an important initial resource for our activities in CDP3 (KRc3.3) to link the multilevel atlas with simulation.

3.7.5 Output 21: Optimised prototype for semi-automatic label propagation across cell-stained histological sections library for microstructure detection and matching

Software component: SGA2 T2.6.4 Semi-automatic interactive tool for cytoarchitectonic brain mapping, ID: 2376

Leader: Timo DICKSCHEID

Based on the work in the first year (C2375), we implemented a fully functional prototype workflow for mapping cytoarchitectonic areas across an unregistered series of consecutive histological sections (C2376). It is a web-based tool which combines editing and display of 2D annotations (using microdraw) with interactive configuration and remote monitoring of Deep Learning training processes on the JURECA supercomputer. Several brain areas were mapped in thousands of consecutive tissue sections by providing expert annotations only in approximately every 100th section. This allowed us to publish the first ultrahigh-resolution full 3D maps of cytoarchitectonic areas in the BigBrain, linked to the knowledge graph (Fig. 12: Area hOc2, area hOc1).

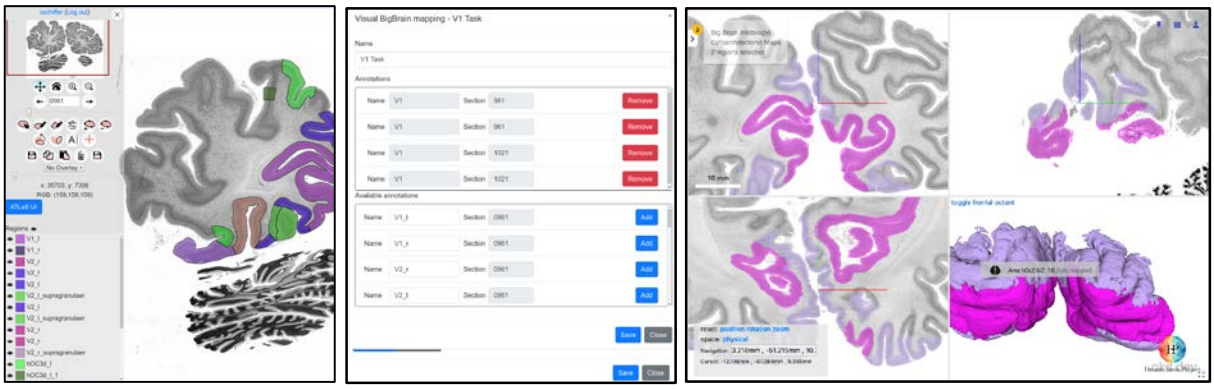

Figure 12: Tool and results for Deep Learning aided cytoarchitectonic mapping.

Left: Interactive annotation of brain areas in a modified version of microdraw (https://microdraw.pasteur.fr). Middle: Controlling training and prediction of automatic segmentations using the web-based workflow. Right: Full 3Dmaps of areas hOc1 and hOc2 produced by the Deep Learning aided workflow in the HBP atlas (https://bigbrain.humanbrainproject.eu).

Table 19: Output 21 Links

Component	Link to	URL
C2376	Software, Technical and User Documentation	https://wiki.ebrains.eu/bin/view/Collabs/cytoarchitectonic-labelpropagation/

3.7.5.1 Actual and Potential Use of Output 21

The mapping tool has been used successfully by neuroanatomists to generate 3D maps of visual areas in the BigBrain model. Some of these maps are now publicly available at https://bigbrain.humanbrainproject.eu, and have been presented to a wider audience at the annual meeting of the organization for human brain mapping (Schiffer et al., OHBM 2019, Rome, E1555).

3.7.6 Output 22: Fibre analysis through large human brain areas

Software component: SGA2 T2.6.4 Fiber analysis though large human brain areas, ID: 2356

Leader: Ludovico SILVESTRI, Giacomo MAZZAMUTO

In addition to the machine-learning algorithm for 3D segmentation and morphochemical classification of neurons (already described in M12 deliverable, D2.7.1, C2354), we developed an automatic software tool to estimate the 3D orientation of myelinated fibers across the sample to analyze images obtained with Two-Photon Fluorescence Microscopy (TPFM, T2.3.4). The software (not curated yet, Table 20) virtually dissects the volume in portions of 60 µm. There, it applies a Structure Tensor (ST) analysis to extract the main direction of the fibers, storing all these orientations as versors across the entire volume, Fractional anisotropy (FA) is also collected for each portion. The versors obtained can be used to calculate the Orientation Distribution Function (ODF) of areas of interest and with that estimate the organization of the fiber thought the volume.

Table 20: Output 22 Links

Component	Link to	URL
C2356	Software Repository	https://github.com/lens-biophotonics/st_fibre_analysis_hbp
	Technical and User Documentation	https://github.com/lens-biophotonics/st_fibre_analysis_hbp/blob/master/README.md

3.7.6.1 Actual and Potential Use of Output 22

The software tool enables to calculate in 3D the fibers orientation allowing the analysis of the large-volume high-resolution data produced by the TPFM. The versors obtained from the tool will enable to compare the fiber orientation obtained with this high-resolution methodology with that obtained with other methodology like 3D-PLI and dMRI.

3.7.7 Output 23: CNN-based sulcus recognition

Software component: SGA2 T2.6.3 Spatial transformation routines for projection of data across templates, ID: 2259

Leader: Jean-Francois MANGIN

The **new** CNN-based sulcus recognition algorithm has been integrated in the BrainVISA toolbox (not curated, Table 21) and applied to HCP (1000 subjects) and UKbiobank (20000 subjects) datasets. An alternative version dedicated to chimps has been designed, trained on 30 subjects with manual sulcus labelling, and applied on an outstanding dataset of over 200 chimps MRI. A third version dedicated to infants is in progress.

Table 21: Output 23 Links

Component	Link to	URL
C2259	Software Repository	https://github.com/brainvisa/morpho-deepsulci
	Technical and User Documentation	https://www.sciencedirect.com/science/article/pii/S1361841520300189?via%3Dihub

3.7.8 Output 24: Aligning great ape template spaces

Software component: SGA2 T2.6.3 Spatial transformation routines for projection of data across templates, ID: 2259

Leader: Jean-Francois MANGIN

The DISCO sulcus-based alignment toolbox (not curated, has been used to create template spaces for several Great Ape species for chimps (60 3T MRI), gorilla (20 postmortem MRI). This work will proceed further with Orang-Utang, Baboon and Macaques. Cross species spatial transformations have been generated using DISCO between the HBP human-based standard spaces and these primate spaces, allowing cross species comparison of various structures (Fig. 13).

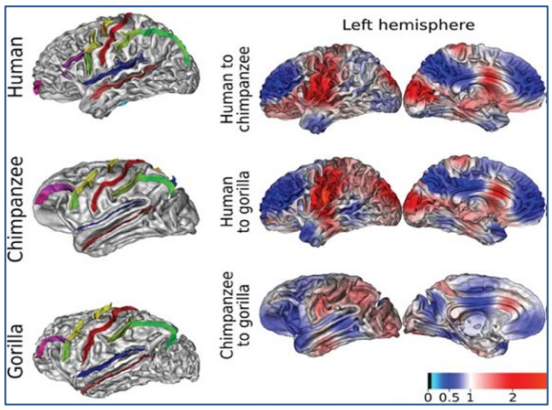

Figure 13: Cross species spatial transformation

Using DISCO to generate a matrix of pairwise spatial transformations between species-specific template spaces.

Table 22: Output 24 Links

Component	Link to	URL
C2259	Software Repository	http://brainvisa.info/axon-4.6/en/processes/disco_pipeline.html
	Technical and User Documentation	http://brainvisa.info/axon-4.6/en/processes/categories/disco/category_documentation.html

3.7.8.1 Actual and Potential Use of Outputs 23, 24

All the datasets with automatically labelled sulci are used to create representations of the variability of the folding patterns in task T2.4.1 (output 11).

The sulcus-based alignment of the chimps is now used to generate the first atlas of the fibre bundles of the chimp, which will be aligned with the human atlas of the HBP for cross species comparisons. Moreover, achieving robust alignment of any subject into the HBP template spaces will have an impact for a medical use of the HBP portal. The main stream strategies, indeed, do not overcome failure of the spatial normalization process used as a preprocessing by most of the brain image analysis pipelines.

3.7.9 Output 25: Objective function for matching images to tissue probability maps

Software component: Objective function for matching images to tissue probability maps, ID: 2577

Leader: John ASHBURNER

The multi-modal alignment delivered by Task 2.6.3 is essential for the multi-modal, multi-scale human brain atlas (KR 2.1). This includes developing an objective function for matching images to tissue probability maps (C2577), which is part of a flexible software framework for diffeomorphic alignment between tissue probability maps and whole-brain 3D images of various types. Some functionality from the SPM12 package was used for this component. The software outperforms SoTA methods based on overlap scores of manually traced brain structures. This was assessed using two publicly available datasets (IBSR18 and LPBA40), and results of one of these are shown in Fig. 14.
To reach users outside the HBP, this toolbox will be incorporated into next major release of the SPM software, which is used by thousands of brain imaging researchers around the world. This will also ensure continued maintenance and improvements to the software (not curated yet, Table 23) after the completion of SGA2.

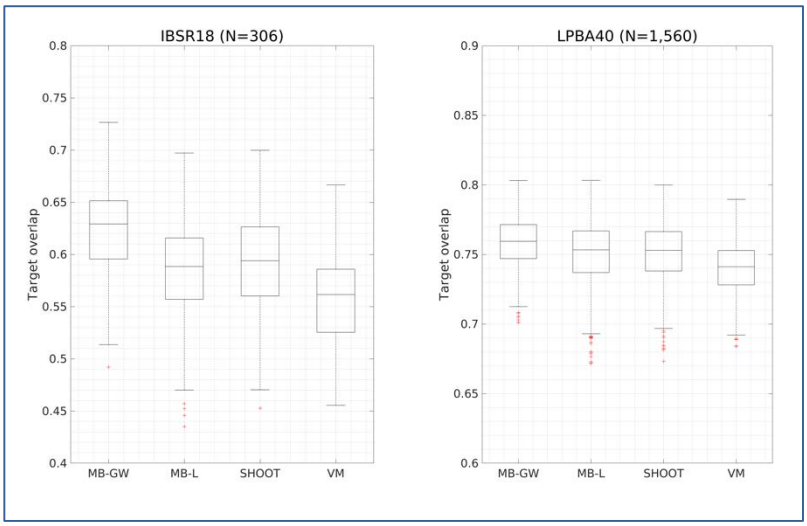

Figure 14: Comparison of multi-modal diffeomorphic image alignment algorithm.

Comparison of multi-modal diffeomorphic image alignment algorithm (C2577 – "Multi-Brain", MB-GW and MB-L) based on overlaps of manually traced brain structures, compared with other state-of-the-art image registration approaches (Shoot and VoxelMorph).

Table 23: Output 25 Links

Component	Link to	URL
C2577	Software Repository	https://github.com/WTCN-computational-anatomy-group/diffeo-segment
	Technical Documentation	https://arxiv.org/pdf/1908.05926.pdf
	User Documentation	https://github.com/WTCN-computational-anatomy-group/diffeo-segment

3.7.10 Output 26: Patch – based Bayesian CCA methods

Software component: Patch-based Bayesian CCA methods, ID: 2579

Leader: John ASHBURNER

Making use of the data generated by the HBP often involves some form of multi-atlas label propagation schemes to automatically define structures on new 3D image volumes. As a faster and more flexible alternative, software for a Bayesian patch-based latent variable method (C2579) was developed for encoding local relationships between tissue-type maps (grey matter, white matter,

etc.) and other image information, such as cytoarchitectonic labels. In combination with more accurate image alignment, this software should enable a diverse variety of MRI scans to be parcellated into different regions using relatively small amounts of training data. The software (not curated, Table 24) is still undergoing validation using manually defined brain parcellations.

Table 24: Output 26 Links

Component	Link to	URL
C2579	Software Repository	https://github.com/WCHN/Label-Training
	Technical Documentation	
	User Documentation	https://github.com/WCHN/Label-Training

3.7.10.1 Actual and Actual and Potential Use of Outputs 25, 26

The Bayesian framework is designed to improve the HBP atlas and align clinical data into the HBP spaces.

3.7.11 Output 27: Enriching the Human Connectome

Dataset component: SGA2 T2.6.7 Online version of von Economo and Koskinas atlas, ID: 3024

Leader: Claus HILGETAG

We defined a virtual 3D von Economo and Koskinas Atlas independent of existing reference geometries, through 3D scanning two individual, well-preserved 3D plaster models of the vEK parcellation manufactured in the era of von Economo. Significant efforts have gone into reconstructing the 3D model and preparing the resulting digital atlas for registration and integration with both The BigBrain atlas as well as The Virtual Brain. The integration of such an atlas demonstrates a successful instance of co-design between the HBP and TVB platforms.

More details in D2.7.1. Dataset are curated but under embargo (Table 25), for publication preparation purposes.

Table 25: Output 27 Links

Component	Link to	URL
C3024	Data Repository, Technical and User Documentation	https://kg.ebrains.eu/search/instances/Project/cf4b19be-725c-4047-a7ac-4f6f6bdb6b8f

3.7.11.1 Actual and Potential Use of Output 27

This output contributes to SP5 (Neuroinformatics) by providing essential brain architecture data to the HBP Atlas and enabling the prediction of fundamental features of human brain connectivity.

Moreover, the output directly contributes to TVB simulation software which has over 25,000 downloads. Within TVB, an interactive web-based atlas viewer was extended to feature the vEK parcellations of the cortex. Beyond the scope of simulations for clinical and scientific use-cases, the web-atlas feature in particular may be used for educational and show-case purposes - supporting the overall educational and outreach mission of EBRAINS.

3.8 Publications KR2.1

3.8.1 Peer-Review

Output 1, C365: Pinho, A. L., Amadon, A., Ruest, T., et al. Individual Brain Charting, a high-resolution fMRI dataset for cognitive mapping. Scientific Data, *5* (2018) (P1408); this publication represents the technical validation of output 1.

Output 2, C2245: Perrone-Bertolotti, M., El Bouzaïdi Tiali, S., Vidal, J. R., et al. A real-time marker of object-based attention in the human brain. A possible component of a "gate-keeping mechanism" performing late attentional selection in the Ventro-Lateral Prefrontal Cortex. *Neuroimage, 210*: 116574. (2020) (P2323); this publication confirms that Output 2 has been validated by scientific peer review.

Holdgraf, C., Appelhoff, S., Bickel, S., et al. "iEEG-BIDS, extending the Brain Imaging Data Structure specification to human intracranial electrophysiology." *Scientific Data, 6.1*: 1-6. (2019) (P2033); this publication contributes to KR2.1, by providing the structural extension to make iEEG datasets more transparent, reusable, and reproducible.

Output 3, C2272, C2319: Grodzinsky, Y., Deschamps, I., Pieperhoff, P., et al. Logical negation mapped onto the brain. *Brain Structure and Function, 225*(1):19-31. (2020) (P2307); this publication confirms that Output 3 has been validated by scientific peer review.

Palomero-Gallagher, N., Zilles, K. Differences in cytoarchitecture of Broca's region between human, ape and macaque brains. *Cortex, 118*: 132-153. (2019) (P1560); this publication confirms that Output 3 has been validated by scientific peer review.

Palomero-Gallagher, N., Hoffstaedter, F., Mohlberg, H., et al. Human pregenual anterior cingulate cortex: structural, functional and connectional heterogeneity. *Cerebral Cortex, 29*: 2552-2574. (2019) (P1328); this publication provides key datasets for Output 3 and confirms that Output 3 has been validated by scientific peer review.

Ruan, J., Bludau, S., Palomero-Gallagher, N., et al. Cytoarchitecture, probability maps, and functions of the human supplementary and pre-supplementary motor areas. *Brain Structure and Function, 223*: 4169-4186. (2018) (P1392); this publication provides key datasets for Output 3 and confirms that Output 3 has been validated by scientific peer review.

Richter, M., Amunts, K., Mohlberg, H., et al. Cytoarchitectonic segregation of human posterior intraparietal and adjacent parieto-occipital sulcus and its relation to visuomotor and cognitive functions. *Cerebral Cortex*, *29*(3): 1305-1327. (2019) (P1629); this publication confirms that Output 3 has been validated by scientific peer review.

Wojtasik, M., Bludau, S., Eickhoff, S. B., et al. Cytoarchitectonic Characterization and Functional Decoding of Four New Areas in the Human Lateral Orbitofrontal Cortex. *Frontiers in Neuroanatomy*, *14*: 2. (2020) (P2432); this publication confirms that Output 3 has been validated by scientific peer review.

Wolf. D., Klasen, M., Eisner, P., et al. Central serotonin modulates neural responses to virtual violent actions in emotion regulation networks. *Brain Structure and Function, 223*: 3327-3345. (2018) (P1375); this publication elaborates on the potential application of the work carried out in Output 3.

Output 4, C2632: Lange, G., Senden, M., Radermacher, A., & De Weerd, P. Interfering with a memory without erasing its trace. *Neural Networks, 121*: 339–355. (2020) (P2053); this publication confirms that Output 4 has been validated by scientific peer review.

Output 7, C2306: Reuter, N., Genon, S., Masouleh, S. K., et al. CBPtools: a Python package for regional connectivity-based parcellation. *Brain Structure and Function (in press)* (P2431-in validation process); this publication represents the technical validation of Output 7.

Eickhoff, S. B., Thomas Yeo, B. T., Genon, S. Imaging-based parcellations of the human brain. Nature Reviews Neuroscience, *19*: 11 (2018) (P1550); this publication contributes to Output 7, by providing insights on connectivity-based parcellation of the human brain.

Output 8, C2315: Palomero-Gallagher, N., Kedo, O., Mohlberg, H., et al. Multimodal mapping and analysis of the cyto-and receptorarchitecture of the human hippocampus. *Brain Structure and Function*, 1-27. (2020) (P2320); this publication confirms that Output 8 has been validated by scientific peer review.

Behuet, S., Cremer, J. N., Cremer, et al. Developmental Changes of Glutamate and GABA Receptor Densities in Wistar Rats. *Frontiers in Neuroanatomy*, *13*: 100. (2019) (P2319); this publication confirms that Output 8 has been validated by scientific peer review.

Mann, T., Karl, Z., Felix, K., et al. Acetylcholine neurotransmitter receptor densities in the striatum of hemiparkinsonian rats following Botulinum neurotoxin-A injection. *Frontiers in Neuroanatomy, 12*: 65. (2018) (P1388); this publication represents the technical validation of the dataset in Output 8.

Antipova, V., Wree, A., Holzmann, C., et al. Unilateral Botulinum neurotoxin-A injection into the striatum of C57BL/6 mice leads to a different motor behavior compared to rats. *Toxins, 10*(7). pii: E295. (2018) (P1846); this publication elaborates on the potential application of the dataset in Output 8.

Output 9, C2312, C2313: Bittner, N., Jockwitz, C., Mühleisen, T. W., et al. (2019). Combining lifestyle risks to disentangle brain structure and functional connectivity differences in older adults. *Nature Communications*, *10*(1): 1-13. (2019) (P1666); this publication confirms that Output 9 has been validated by peer review.

Masouleh, S. K., Eickhoff, S. B., Hoffstaedter, F., et al. Empirical examination of the replicability of associations between brain structure and psychological variables. *Elife*, *8*: e43464. (2019) (P1777); this publication confirms that Output 9 has been validated by peer review.

Weis, S., Patil, K. R., Hoffstaedter, F., et al. Sex classification by resting state brain connectivity. *Cerebral Cortex*, *30*(2): 824-835. (2020) (P2034); this publication confirms that Output 9 has been validated by scientific peer review.

Heim, S., Stumme, J., Bittner, N., et al. Bilingualism and "brain reserve": a matter of age. *Neurobiology of Aging*, *81*: 157-165. (2019) (P2037); this publication confirms that Output 9 has been validated by peer review.

Jockwitz, C., Mérillat, S., Liem, F., et al. Generalizing age effects on brain structure and cognition: A two-study comparison approach. *Human Brain Mapping*, *40*(8): 2305-2319. (2019) (P1644); this publication confirms that Output 9 has been validated by peer review.

Stumme, J., Jockwitz, C., Hoffstaedter, F., et al. Functional network reorganization in older adults: Graph-theoretical analyses of age, cognition and sex. *Neuroimage*, 116756. (2020) (P2488); this publication confirms that Output 9 has been validated by peer review.

Tahmasian M, Sepehry AA, Samea F, et al. Practical recommendations to conduct a neuroimaging meta-analysis for neuropsychiatric disorders. *Human Brain Mapping*, *40*(17): 5142-5154. (2019) (P2203); this publication contributes to Output 9, by providing insights on the replicability of neuroimaging studies.

Output 10, C2314: Grasby, K. L., Jahanshad, N., Painter, J. N., et al. The genetic architecture of the human cerebral cortex. *Science*, *367*: 6484. (2020) (P2542); this publication confirms that Output 10 has been validated by peer review.

Caspers, S., Röckner, M. E., Jockwitz, et al. Pathway-Specific Genetic Risk for Alzheimer's Disease Differentiates Regional Patterns of Cortical Atrophy in Older Adults. *Cerebral Cortex, 30*(2): 801-811. (2020) (P2065); this publication contributes to Output 10 and KR2.1, by providing insights on the relation genotype - brain variability.

Rubbert, C., Mathys, C., Jockwitz, C., et al. Dose response of the 16p11. 2 distal copy number variant on intracranial volume and basal ganglia. *Molecular Psychiatry*, 1-19. (2019) (P1652); this publication contributes to Output 10 and KR2.1, by providing insights on the relation genotype - brain variability.

Output 11, C2362: Mangin, J. F., Le Guen, Y., Labra, N., et al. "Plis de passage" Deserve a Role in Models of the Cortical Folding Process. *Brain Topography, 32*: 1035–1048 (2019) (P2198-in validation process); this publication contributes to Output 11, by providing insights on models of cortical folding.

Sarrazin, S., Cachia, A., Hozer, F., et al. Neurodevelopmental subtypes of bipolar disorder are related to cortical folding patterns: An international multicenter study. *Bipolar Disorders, 20*: 721-732. (2018) (P1377); this publication contributes to output 11 by assessing the folding power of the cortex in patients with bipolar disorders.

Output 14, C2345: Qi, G., Yang, D., Ding, C., & Feldmeyer, D. Unveiling the Synaptic Function and Structure Using Paired Recordings From Synaptically Coupled Neurons. *Frontiers in Synaptic Neuroscience*, *12*: 5. (2020) (P2399); this publication highlights the benefits of the technology used to generate Output 14.

Output 15, C2318: Impieri D, Zilles K, Niu M, et al. Receptor density pattern confirms and enhances the anatomic-functional features of the macaque superior parietal lobule areas. *Brain Structure and Function, 224*: 2733-2756. (2019) (P2063); this publication provides the technical validation of Output 15.

Output 16, C2470, C2322: Arsenault, J. T., & Vanduffel, W. Ventral midbrain stimulation induces perceptual learning and cortical plasticity in primates. *Nature Communications*, *10*(1): 1-13. (2019) (P2064); this publication confirms that the work carried out here has been validated by scientific peer review.
Zhu, Q., & Vanduffel, W. Submillimeter fMRI reveals a layout of dorsal visual cortex in macaques, remarkably similar to New World monkeys. *Proceedings of the National Academy of Sciences*, *116*(6): 2306-2311. (2019) (P1645); this publication utilizes analytical tools developed to carry out Output 16.

Output 20, C2271: Dickscheid T, Haas S, Bludau S, et al. Towards 3D Reconstruction of Neuronal Cell Distributions from Histological Human Brain Sections. *Advances in Parallel Computing*, *34* (Future Trends of HPC in a Disruptive Scenario):223–239. (2019) (P2376); this publication represents the technical validation of the work carried out in Output 20.

Output 23, C2259: Borne, L., Rivière, D., Mancip, M., et al. Automatic labeling of cortical sulci using patch- or CNN-based segmentation techniques combined with bottom-up geometric constraints. *Medical Image Analysis*, 101651. (2020) (P2435); this publication represents the technical validation of Output 23.

Output 24, C2259: Ing, A., Sämann, P. G., Chu, C., et al. Identification of neurobehavioural symptom groups based on shared brain mechanisms. *Nature Human Behaviour*, *3*(12): 1306-1318. (2019) (P2218); this publication elaborates on the potential application of Output 24.

3.8.2 Pre-Print

Output 10, C2314: Valk, S. L., Xu, T., Masouleh, Goulas, A., et al. Shaping brain structure: Genetic and phylogenetic axes of macro scale organization of cortical thickness. *bioRxiv* (2020) (P2375); this publication represents the technical validation of Output 10.

Output 14, C2345: Ding, C., Emmenegger, V., Schaffrath, K., et al. Layer-specific inhibitory microcircuits of layer 6 interneurons in rat prefrontal cortex. *bioRxiv* (2020) (P2378); this publication complements the validation of Output 14.

Yang, D., Günter, R., Qi, G., et al. Cell Type-Specific Modulation of Layer 6A Excitatory Microcircuits by Acetylcholine in Rat Barrel Cortex. *bioRxiv* (2019) (P2118); this publication complements the validation of Output 14.

Output 21, C2376: Wagstyl, K., Larocque, S., Cucurull, G., et al. BigBrain 3D atlas of cortical layers: cortical and laminar thickness gradients diverge in sensory and motor cortices. *bioRxiv* (2019) (P2332), now accepted in *PLoS Biology*, *18*(4): e3000678. (2020); this publication elaborates on the potential application of the work carried out in Output 21.

3.8.3 Dataset DOI

Output 1, C365: Pinho, A., Amadon, A., Ruest, T. et al. I*ndividual Brain Charting, a high*-resolution fMRI dataset for cognitive mapping. Sci Data 5, 180105 (2018). https://doi.org/10.1038/sdata.2018.105 (P1408).

Output 3, C2319, C2272: Amunts, K., Eickhoff, S. B., Caspers, S., et al. (2019). *Whole-brain parcellation of the JuBrain Cytoarchitectonic Atlas (v18)* [Data set]. Human Brain Project Neuroinformatics Platform. DOI: 10.25493/8EGG-ZAR

Amunts, K., Iannilli, F., Bludau, S., & Mohlberg, H. (2019). *Probabilistic cytoarchitectonic map of Area Id7 (Insula) (v6.0)* [Data set]. Human Brain Project Neuroinformatics Platform. DOI: 10.25493/B2E3-JQR

Amunts, K., Iannilli, F., Bludau, S., & Mohlberg, H. (2019). *Probabilistic cytoarchitectonic map of Area Id7 (Insula) (v6.1)* [Data set]. Human Brain Project Neuroinformatics Platform. DOI: 10.25493/88QG-JMS

Amunts, K., Kedo, O., Kindler, M., et al. (2019). *Probabilistic cytoarchitectonic map of CA (Hippocampus) (v11.1)* [Data set]. Human Brain Project Neuroinformatics Platform. DOI: 10.25493/B85T-D88

Saal, M., Bludau, S., Mohlberg, H., et al. (2019). *Probabilistic cytoarchitectonic map of Area OP8 (Frontal Operculum) (v5.0)* [Data set]. Human Brain Project Neuroinformatics Platform. DOI: 10.25493/1NGE-YH3

Saal, M., Bludau, S., Mohlberg, H., et al. (2019). *Probabilistic cytoarchitectonic map of Area OP8 (Frontal Operculum) (v5.1)* [Data set]. Human Brain Project Neuroinformatics Platform. DOI: 10.25493/NGF8-TA4

Saal, M., Bludau, S., Mohlberg, H., et al. (2019). *Probabilistic cytoarchitectonic map of Area OP9 (Frontal Operculum) (v5.0)* [Data set]. Human Brain Project Neuroinformatics Platform. DOI: 10.25493/QYFC-TQV

Saal, M., Bludau, S., Mohlberg, H., et al. (2019). *Probabilistic cytoarchitectonic map of Area OP9 (Frontal Operculum) (v5.1)* [Data set]. Human Brain Project Neuroinformatics Platform. DOI: 10.25493/3A30-5E4

Wojtasik, M., Mohlberg, H., & Amunts, K. (2019). *Probabilistic cytoarchitectonic map of Area Fo4 (OFC) (v2.1)* [Data set]. Human Brain Project Neuroinformatics Platform. DOI: 10.25493/29G0-66F

Wojtasik, M., Mohlberg, H., & Amunts, K. (2019). *Probabilistic cytoarchitectonic map of Area Fo5 (OFC) (v2.1)* [Data set]. Human Brain Project Neuroinformatics Platform. DOI: 10.25493/HJMY-ZZP

Wojtasik, M., Mohlberg, H., & Amunts, K. (2019). *Probabilistic cytoarchitectonic map of Area Fo6 (OFC) (v2.1)* [Data set]. Human Brain Project Neuroinformatics Platform. DOI: 10.25493/34Q4-H62

Wojtasik, M., Mohlberg, H., & Amunts, K. (2019). *Probabilistic cytoarchitectonic map of Area Fo7 (OFC) (v2.1)* [Data set]. Human Brain Project Neuroinformatics Platform. DOI: 10.25493/3WEV-561

Zachlod, D., Bludau, S., Mohlberg, H., & Amunts, K. (2019). *Probabilistic cytoarchitectonic map of Area STS1 (STS) (v3.0)* [Data set]. Human Brain Project Neuroinformatics Platform. DOI: 10.25493/2G11-1WA

Zachlod, D., Bludau, S., Mohlberg, H., & Amunts, K. (2019). *Probabilistic cytoarchitectonic map of Area STS1 (STS) (v3.1)* [Data set]. Human Brain Project Neuroinformatics Platform. DOI: 10.25493/F6DF-H8P

Zachlod, D., Bludau, S., Mohlberg, H., & Amunts, K. (2019). *Probabilistic cytoarchitectonic map of Area STS2 (STS) (v3.0)* [Data set]. Human Brain Project Neuroinformatics Platform. DOI: 10.25493/Y5QZ-KV

Zachlod, D., Bludau, S., Mohlberg, H., & Amunts, K. (2019). *Probabilistic cytoarchitectonic map of Area STS2 (STS) (v3.1)* [Data set]. Human Brain Project Neuroinformatics Platform. DOI: 10.25493/KHY9-J3Y

Zachlod, D., Rüttgers, B., Bludau, S., et al. (2019). *Probabilistic cytoarchitectonic map of Area TeI (STG) (v5.1)* [Data set]. Human Brain Project Neuroinformatics Platform. DOI: 10.25493/DTC3-EVM

Zachlod, D., Rüttgers, B., Bludau, S., et al. (2019). *Probabilistic cytoarchitectonic map of Area TI (STG) (v5.1)* [Data set]. Human Brain Project Neuroinformatics Platform. DOI: 10.25493/57FA-VX6

Zachlod, D., Morosan, P., Bludau, S., et al. (2019). *Probabilistic cytoarchitectonic map of Area TE 2.1 (STG) (v5.1)* [Data set]. Human Brain Project Neuroinformatics Platform. DOI: 10.25493/R28N-2TD

Zachlod, D., Morosan, P., Bludau, S., et al. (2019). *Probabilistic cytoarchitectonic map of Area TE 2.2 (STG) (v5.1)* [Data set]. Human Brain Project Neuroinformatics Platform. DOI: 10.25493/RTTN-R5F

Output 8, C2315: Palomero-Gallagher, N., Zilles, K. (2020). Density measurements of different receptors for CA1 (Hippocampus) [human, v2.0]. Human Brain Project Neuroinformatics Platform. DOI: 10.25493%2FY7YV-6Q6

Palomero-Gallagher, N., Zilles, K. (2020). Density measurements of different receptors for CA2 (Hippocampus) [human, v2.0]. Human Brain Project Neuroinformatics Platform. DOI: 10.25493%2F4F4S-W5A

Palomero-Gallagher, N., Zilles, K. (2020). Density measurements of different receptors for CA3 (Hippocampus) [human, v2.0]. Human Brain Project Neuroinformatics Platform. DOI: 10.25493%2FXFHR-X41

Palomero-Gallagher, N., Zilles, K. (2020). Density measurements of different receptors for DG (Hippocampus) [human, v2.0]. Human Brain Project Neuroinformatics Platform. DOI: 10.25493%2FM8PK-C82

Palomero-Gallagher, N., Zilles, K. (2020). Density measurements of different receptors for stratum cellulare of CA (Hippocampus) [human, v2.0]. Human Brain Project Neuroinformatics Platform. DOI: 10.25493%2F9DDZ-SJP

Palomero-Gallagher, N., Zilles, K. (2020). Density measurements of different receptors for stratum moleculare of CA (Hippocampus) [human, v2.0]. Human Brain Project Neuroinformatics Platform. DOI: 10.25493%2FKYZ2-4GM

Output 15, C2318: Palomero-Gallagher, N., Zilles, K. (2020). Density measurements of different receptors for dorsal part of Area hOc2 (V2, 18). Human Brain Project Neuroinformatics Platform. DOI: 10.25493%2FZJ7E-KXZ

Palomero-Gallagher, N., Zilles, K. (2020). Density measurements of different receptors for ventral part of Area hOc2 (V2, 18) [human, v1.0]. Human Brain Project Neuroinformatics Platform. DOI: 10.25493%2F2E5C-PVM

Palomero-Gallagher, N., Zilles, K. (2020). Density measurements of different receptors for dorsal part of Area hOc3 (Cuneus) [human, v1.0]. Human Brain Project Neuroinformatics Platform. DOI: 10.25493%2F4ETW-9XB

Palomero-Gallagher, N., Zilles, K. (2020). Density measurements of different receptors for ventral part of Area hOc3 (LingG) [human, v1.0]. Human Brain Project Neuroinformatics Platform. DOI: 10.25493%2FTBMX-BZ9

4. Key Result KR2.2: High - resolution reconstruction of nerve fibre architecture applying 3 different imaging techniques in the same brain sample

The main goal was to enable new insights into the micro-to-macro organization of the complex, nested fiber architecture in the human brain, with focus on the hippocampus. Three different label-free neuroimaging techniques were optimized to provide complementary contrasts in the same tissue sample: magnetic resonance imaging (MRI), 3D polarized light imaging (3D-PLI), and two-photon fluorescence microscopy (TPFM). We have developed unique brain preparations and new measurement protocols (e.g., MAGIC), rendering joint tissue imaging possible, as well as image processing pipelines for technique specific signal interpretation and co-alignment. In parallel to the time-consuming high-resolution measurements pushing all three techniques towards their limits, software packages for the modeling of fiber pathways and fiber orientation distributions have been realized by means of simulation approaches, to understand and leverage synergies between different measurements. All software implementations have been done in view of new hardware developments and increasing brain tissue volumes to be addressed in SGA3. Building on the gained experiences with the joint hippocampus sample, new large-scale cutting-edge data acquisitions with have already been started and delivered (e.g., MRI data of an entire 'Chenonceau' human brain and light sheet fluorescence microscopy (LSFM) of an entire hippocampus).

4.1 Overview of Outputs contributing to the Key Result

Below the list of SP2 outputs contributing to this KR, for more details see below.

Output number	Component	Name
1	C2386	Dataset of human hippocampus based on joint Diffusion MRI and 3D Polarized Light Imaging acquisitions
2	C2367	HPC-based global tractography
3	C2387	Combined application of Two-Photon Fluorescence Microscopy and 3D Polarized Light Imaging to the same section samples
4	C2388	Dataset of human hippocampus based on joint Diffusion MRI and 3D Polarized Light Imaging, and Two-Photon-Fluorescence Microscopy acquisitions
5	C2366	Fiber Architecture Simulation Toolbox for 3D-PLI (fastpli)
6	C2293	3D reconstruction of a whole left human hippocampus at microscopic resolution
7	C2361	Acquisition of mesoscopic scale UHF MRI dataset on the Chenonceau brain

4.1.1 How Outputs How outputs relate to each other and the Key Result

Outputs 1 and 4 build the key dataset for KR2.2 providing true multi-modality multi-scale insights into the same hippocampus sample. More than 10,795 files were acquired, assembled, analyzed, registered, and curated. The entire hippocampus was scanned by means of anatomical and diffusion MRI sequences, as well as with 3D-PLI section-by-section. Ultra-high TPFM measurements finally enriched the dataset in selected brain sections. In order to realize the serial application of 3D-PLI and TPFM without using any kind of exogenous labeling or staining, the MAGIC protocol was successfully developed which intentionally increases the auto-fluorescence of myelinated fibers in 3D-PLI prepared brain sections (output 3). Output 2 is a tool for global tractography that has been initially developed and optimized to analyze the structural connectivity in diffusion MRI data. It turned out to be suited for 3D-PLI orientation data as well. Output 5 is a software package for modeling of nerve fiber structures and their (simulated) measurements in a tilting 3D-PLI microscope. Combined with the (earlier in SGA2) delivered MEDUSA toolkit and a Monte-Carlo-based diffusion simulator, the responses of 3D-PLI and diffusion MRI to the same underlying (known) fiber arrangements can be studied now. This significantly improves the understanding of measurements in a joint experiment, Output 6 highlights the great potential of cutting-edge LFSM to address larger tissue volumes as compared to TPFM. The delivered hippocampus data originate from a different tissue sample as used for outputs 1-4, but they will be integrated into the same reference space in future. Finally, multi-modal, nested connectome analysis of the entire human brain is of outmost interest to the community and represents a main research topic in SGA3. To address this aspect early on, an entire human brain (referred to as Chenonceau brain) has been MRI scanned (output 7).

4.1.2 Output 1: Dataset of human hippocampus based on joint Diffusion MRI and 3D Polarized Light Imaging acquisitions

Dataset components: SGA2 T2.3.3 Fibre architecture reconstruction with dMRI and 3D-PLI, ID: 2386

Leader: Markus AXER, Cyril POUPON

We provide ground-breaking insights into the micro-to-macro organization of the complex fiber architecture in the human hippocampus (KR2.2). The assembled dataset originates from serial measurements of a whole hippocampus using post-mortem anatomical and Diffusion MRI (dMRI) and 3D Polarized Light Imaging (3D-PLI), based on our work started in SGA1. MRI scanning was performed

with a 11.7 T Preclinical MRI system yielding T1-w and T2-w maps at 150 μm and dMRI-based maps at 300 μm resolution. During tissue sectioning (60 μm thickness) blockface images were acquired from the surface of the frozen brain block, serving as reference for data integration. All multimodal, multiscale data were co-aligned with each other using (non-)linear registration (Fig. 15, top row). Utilizing VOLUBA as part of the EBRAINS human brain atlas services, the hippocampus dataset was anchored to the BigBrain space in a linear, manual way (Fig. 15, bottom row). It is the very first large-scale, high-resolution, multimodal dataset visualized. Data and method publications are currently in preparation, and under embargo (curated, Table 26).

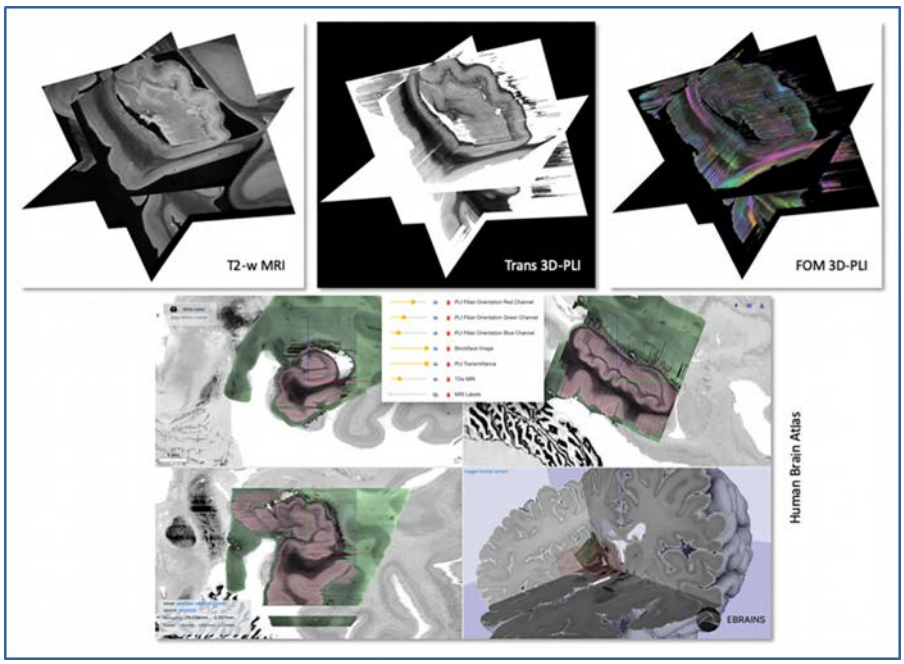

Figure 15: Cross-alignment of MRI-based measurements and 3D-PLI modalities

MRI-based measurements and 3D-PLI modalities were cross-aligned to each other (top row) and anchored with the interactive tool VOLUBA into the BigBrain template as provided by the EBRAINS human brain atlas services.

Table 26: Output 1 Links

Component	Link to	URL
C2386	Data Repository, Technical and User Documentation	http://doi.org/10.25493/JQ30-E08

4.1.2.1 Actual and Potential Use of Output 1

The combined datasets are used by HBP partners to compare nerve fiber orientations derived from the complementary imaging methods, in order to describe and quantify nested connectome characteristics in the hippocampus (T2.3.4). Specific efforts are currently being made to adapt global dMRI tractography algorithms to the specific requirements set by 3D-PLI data (output 2). In addition, a first study was carried out to quantify the uncertainty of fiber orientation estimations from 3D-PLI data (P2531). The hippocampus data provide the ideal test environment for such issues. They also address the external HBP community of tractography developers, which are often lacking histological high-resolution volume data for validation purposes.
It is the first time that large-scale 3D-PLI data become publicly available and enrich the EBRAINS human brain atlas with new modalities. This unique dataset represents a perfect use case to carry out multimodal structural analysis in an atlas environment. Within HBP, it helps to define and develop algorithms to align high-resolution, large-scale volumes with the BigBrain reference space (SGA3).

4.1.3 Output 2: Global tractography tool for high resolution dMRI

Software component: SGA2 T2.6.6 HPC compatible global tractography, ID: 2367

Leader: Cyril POUPON, Markus AXER

A novel spin-glass-based global tractography algorithm has been released on the GitLab repository of the NeuroSpin/Ginkgo team that allows to perform fiber tracking using a global optimization of the ill-posed problem consisting in the inference of the connectivity from the observation of a field of local orientation distribution functions (ODF). More details in deliverable D2.7.1. This software is not curated yet.

Table 27: Output 2 Links

Component	Link to	URL
C2367	Software Repository	https://framagit.org/cpoupon/gkg/-/tree/master/dmri%2Fsrc%2Flibrary%2Fgkg-dmri-global-tractography
	Technical and User Documentation	https://framagit.org/cpoupon/gkg/-/issues/1

4.1.3.1 Actual and Potential Use of Output 2

This tool will be used to process the mesoscopic diffusion MRI dataset acquired in the frame of Task 2.1.3, and the whole brain microscopic 3D-PLI dataset to be acquired in the frame of SGA3.

4.1.4 Output 3: Combined application of Two-Photon Fluorescence Microscopy and 3D Polarized Light Imaging to the same section samples

Report component: SGA2 T2.3.4 Combined application of TPFM, 3D-PLI, and dMRI to the same sample, ID: 2387

Component Leader: Markus AXER, Irene COSTANTINI

The application of comprehensive microscopic techniques addressing different spatial scales to the same brain tissue sample is challenging. We have developed a special protocol (MAGIC: Myelin Autofluorescence imaging by Glycerol Induced Contrast enhancement) enabling 3D reconstruction of myelinated fibers within brain sections without exogenous labelling, solely utilizing the emerging myelin autofluorescence (Fig. 16, top). By this means an unstained, formalin fixed, and Glycerol embedded brain section can be imaged successively with 3D-PLI and Two-Photon Fluorescence Microscopy (TPFM). The resulting data are available under the same link as defined in outputs 1, 4.

Table 28: Output 3 Links

Component	Link to	URL
C2387	Report Repository	http://doi.org/10.25493/JQ30-E08

4.1.5 Output 4: Dataset of human hippocampus based on joint MRI and 3D Polarized Light Imaging, and Two-Photon-Fluorescence Microscopy acquisitions

Dataset components: SGA2 T2.3.4 Mapping of fibers and fiber tracts revealed by TPFM, 3D-PLI, and dMRI in the same sample, ID: 2388

Leader: Markus AXER, Irene COSTANTINI, Cyril POUPON

We provide ground-breaking insights into the micro-to-macro organization of the complex fibre architecture in the human hippocampus (KR2.2). As an extension to the output 1 (C2386), we enriched the MRI/3D-PLI datasets with ultra-high resolution TPFM acquisitions of selected sections utilizing the MAGIC protocol. The TPFM measurements provide at 0.44 μm x 0.44 μm x 1 μm resolution unrivalled, 3D insights into the fiber architecture. Non-linear registration to the respective 3D-PLI images enabled first HBP-specific correlation analysis of fiber orientations (Fig. 16, bottom, right).
Data under temporary embargo. The output data (curated) obtained in the context of component C2388 have been added to the same container as defined for output 1, since the brain sample was the same (Table 29).

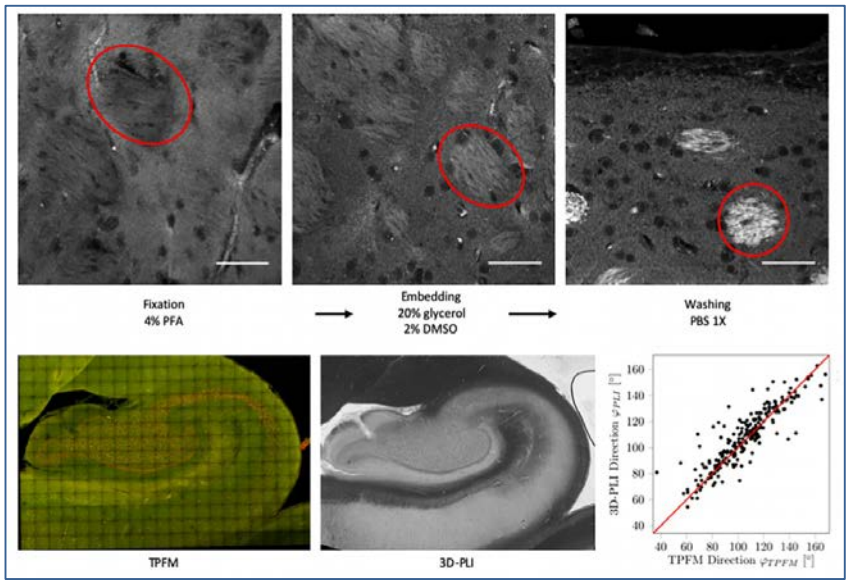

Figure 16: MAGIC protocol applied to a brain section used for 3D-PLI imaging.

The emerging autofluorescence is clearly visible (red circles, top row). 3D-PLI and TPFM can be done on the same tissue (bottom row). Correlative fiber orientation analysis demonstrates good agreement (bottom right).

Table 29: Output 4 Links

Component	Link to	URL
C2388	Data Repository, Technical and User Documentation	http://doi.org/10.25493/JQ30-E08

4.1.5.1 Actual and Potential Use of Outputs 3, 4

The brain preparation protocols for sequential dMRI, 3D-PLI, and TPFM imaging (including MAGIC) are currently applied to different species (rodents, human and non-human primates). In SGA3, methods and workflows as developed in SGA2 (T2.1.3, T2.3.3, T2.3.4, T2.6.6) will be pushed to their limits by addressing an entire human brain. The generated hippocampus datasets are unique and, therefore, HBP-specific. They open up new ways to drive connectivity analysis from micro- to macroscale. Applying methods and workflows which were specifically developed to enable outputs 1,3,4, a study of the birds' hippocampal fiber architecture was successfully carried out (P2224).

4.1.6 Output 5: Fiber Architecture Simulation Toolbox for 3D-PLI (fastPLI)

Software component: SGA2 T2.6.5 Simulator of polarized light and water diffusion in biological tissues, ID: 2366

Leader: Markus AXER, Cyril POUPON

fastPLI is based on Python and offers software packages (modules) to efficiently generate models of collision-free nerve fiber structures (P2541), their simulated measurements in a tilting 3D-PLI microscope setup, and basic analysis of local fiber orientations (P2530). It is the first open source package that allows to investigate birefringence effects in brain tissue and to more accurately understand real 3D-PLI measurements. *fastPLI* is designed to use comprehensive brain tissue models generated by the *FAConstructor (*P2062*)* or *MEDUSA (*P1775), thus paving the way to study and leverage synergies between 3D-PLI and Diffusion MRI measurements (Fig. 17). Software publication of *fastPLI* is currently in preparation, which explains the temporary embargo on the delivered software (not curated, Table 30).

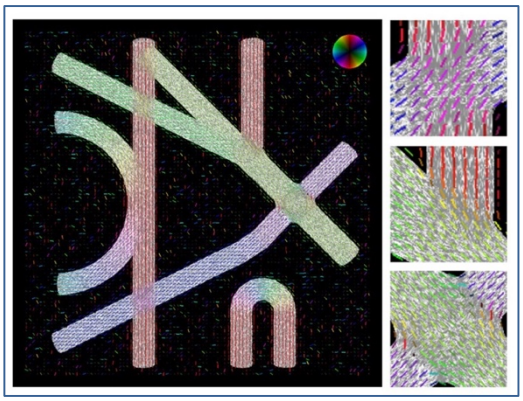

Figure 17: Output 5 example.

Vector field obtained from *fastPLI* simulations of the collision-free Fiber Cup phantom (generated with *FAConstructor*, Reuter et al, 2019, P2062) and overlaid with the employed fiber model. Different fiber orientations/vectors are differently color-coded to simplify visual inspection.

Table 30: Output 5 Links

Component	Link to	URL
C2366	Software Repository	https://github.com/3d-pli/fastpli https://github.com/3d-pli/fastpli/wiki
	Technical and User Documentation	https://github.com/3d-pli/fastpli/wiki

4.1.6.1 Actual and Potential Use of Output 5

Fiber models and derived fiber orientations are important for validating statistics-based analysis (e.g., ODF computation) across Diffusion MRI, 3D-PLI and TPFM modalities (T2.3.3 and T2.3.4). New research has started on simulation-based machine learning approaches to better understand real (in particular small) 3D-PLI signals in complex brain regions, e.g. in the neighborhood of u-fiber systems. Datasets assembled in T2.1.3 appear to be well suited to address this issue in SGA3. Last but not least, *fastPLI* has been proven to be valuable for educational courses, exhibitions and lectures, due to its intuitive usage (according to untrained students). For external HBP users, the toolbox is of interest in the context of tractography developments and validation.
Menzel et al., Physical Review X, (2020, *in press,* P2530) have built upon the fiber models generated with *fastPLI* and developed a simulation framework that permitted the study of transmission microscopy measurements—in particular, light scattering—on large-scale complex fiber structures, using finite-difference time-domain (FDTD) simulations and high-performance computing.

4.1.7 Output 6: 3D reconstruction of a whole left human hippocampus at microscopic resolution

Dataset component: SGA2 - T2.3.1 Layer-specific excitatory and inhibitory neuronal maps of hippocampus, ID: 2293

Leader: Francesco Saverio PAVONE, Irene COSTANTINI

A left post-mortem human hippocampus was cut into 72 slices of 500 µm thickness. Each slice was cleared with the SWITCH/TDE method (Costantini, et al, Biomedical Optics Express, 2019, P2197-in validation process) and labelled with a double staining using an anti-NeuN antibody (to the detect the all neurons) and an anti-GAD67 antibody (to detect inhibitory neurons) (Fig. 18). 3D imaging of the slices has been performed using a custom-made dual view inverted light sheet fluorescence microscope (LSFM) with a resolution of 1.1 x 1.1 x 3.8 µm3. The dataset is the first of its kind and gives the morphological characterization of the human hippocampus at high resolution, permitting a distribution analysis of excitatory and inhibitory neurons. The combination of the clearing procedure and advanced optical technique allowed to bridge the microscopic and the mesoscopic scale overcoming the limitation of conventional techniques. Datasets have been curated but under embargo. Datasets have been curated but under embargo (Table 31).

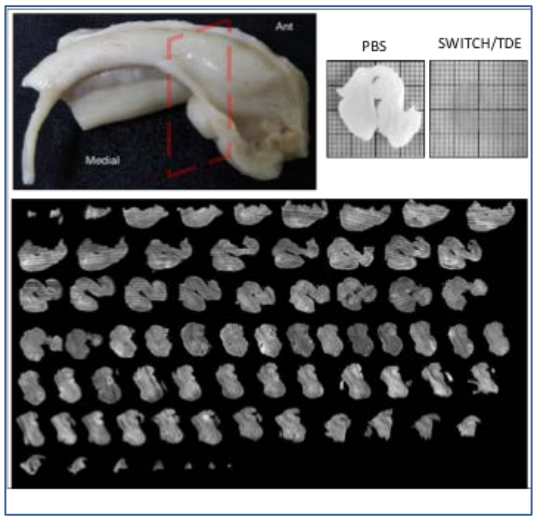

Figure 18: The 3D imaging of the SWITCH/TDE - treated slices.

On the top left: picture of the sample before the cutting. On the right a representative slice before and after the SWITCH/TDE clearing. On the bottom: maximum intensity projection of the 72 slices acquired with the inverted LSFM

Table 31: Output 6 Links

Component	Link to	URL
C2293	Data Repository, Technical and User Documentation	https://kg.ebrains.eu/search/instances/Dataset/8fcf6fa9-deee-492b-be38-f948a8981eda

4.1.7.1 Actual and Potential Use of Output 6

The images are currently under analysis with the automated tools designed in task 2.6.4 to obtain the neuronal segmentation of the two classes in order to have the distribution of the excitatory and inhibitory neurons (in terms of total number, volumes, shapes) in the different layer of the hippocampus. Moreover, the 3D maps data obtained from the reconstruction of excitatory and inhibitory neurons of the hippocampus will be align to the Big Brain reference space and will serve as input to simulate brain states in SGA3.

Output 7: Acquisition of mesoscopic scale UHF MRI dataset on the Chenonceau brain

Dataset component: SGA2 T2.1.3 Ultra high-resolution post mortem diffusion MRI, ID: 2361

Leader: Cyril POUPON

During the first year of SGA2, our team acquired a post-mortem ultra-High Field 11.7T MRI mesoscopic dataset over an entire left hemisphere (called Chenonceau) provided by Christophe DESTRIEUX (CHU Tours, INSERM iBrain). The acquisition of this dataset covers an entire human brain specimen, scanned using anatomical, quantitative and diffusion MRI imaging protocols on a preclinical Bruker 11.7T MRI system, and corresponding to 6000 hours of acquisition in total. More details in deliverable D2.7.1.

Dataset are curated but under embargo (Table 32).

Table 32: Output 7 Links

Component	Link to	URL
C2361	Data Repository, Technical and User Documentation	https://kg.ebrains.eu/search/instances/Dataset/1be7069f-fd40-4f15-b3b3-80904d95e360

4.1.7.2 Actual and Potential Use of Output 7

Because the mesoscopic UHF diffusion MRI dataset is unique in the field of diffusion MRI, generally limited to the millimeter resolution, it establishes a bridge between the microscopic scale of optical methods and the macroscopic scale of *in vivo* imaging methods, thus opening a large range of applications from the enhancement of diffusion conventional and microstructural MRI models and fiber tracking methods to the more fundamental inference of the fine brain connectivity in humans.

4.2 Publications KR2.2

4.2.1 Peer-Review

Output 1, C2387: Schmitz, D., Lippert, T., Amunts, K. & Axer, M. Quantification of fiber fiber orientation uncertainty in polarized light imaging of the human brain, in *Medical Imaging 2020: Physics of Medical Imaging, 1131239.* (2020) (P2531); this publication validates the work carried out in Output 1.

Output 3-4, C2388: Herold C, Schlömer P, Mafoppa-Fomat I, et al. The hippocampus of birds in a view of evolutionary connectomics. *Cortex*, *118*: 165–187. (2019) (P2224); this publication elaborates on the application of workflows and methods developed in Outputs 3, 4, and it extends the cross-species studies of the hippocampus.

Output 5, C2366: Menzel M, Axer M, De Raedt H, et al. Toward a High-Resolution Reconstruction of 3D Nerve Fiber Architectures and Crossings in the Brain Using Light Scattering Measurements and Finite-Difference Time-Domain Simulations. *Physical Review X 10*: 021002 (2020, *in press*) (P2530); this publication describes an essential use case of Output 5 and provides its technical validation.

Reuter, J. A., Matuschke, F., Menzel, M., et al. FAConstructor: an interactive tool for geometric modeling of nerve fiber architectures in the brain. *International Journal of Computer Assisted Radiology and Surgery*, *14*(11), 1881-1889. (2019) (P2062); this publication describes software modules of Output 5 and highlights its usability for simulated polarization microscopy.

Ginsburger, K., Matuschke, F., Poupon, F., et al. MEDUSA: A GPU-based tool to create realistic phantoms of the brain microstructure using tiny spheres. *NeuroImage*, *193*: 10-24. (2019) (P1775); this publication describes software modules of Output 5 and highlights its usability for simulated MRI.

Output 6, C2293: Gavryusev, V., Sancataldo, G., Ricci, P., et al. Dual-beam confocal light-sheet microscopy via flexible acousto-optic deflector. *Journal of Biomedical Optics*, *24*(10): 106504. (2019) (P2305); this publication describes the technical setup used to generate Output 6.

4.2.2 Pre-Print

Output 5, C2366: Matuschke, F., Ginsburger, K., Poupon, C., et al. Dense Fiber Modeling for 3D-Polarized Light Imaging Simulations. (2019) (P2541); this publication, now accepted as book chapter (Springer), describes a specific feature of Output 5, i.e. the dissolving of fiber collisions in tissue models.

4.2.3 Dataset DOI

Output 1,3,4, C2386, C2387, C2388: Axer, M., Poupon, C., & Costantini, I. (2020). *Fiber structures of a human hippocampus based on joint DMRI, 3D-PLI, and TPFM acquisitions* [Data set]. Human Brain Project Neuroinformatics Platform. DOI: 10.25493/JQ30-E08 . Note, this dataset includes about 10,759 individual image files!

5. Conclusions

SP2's work in SGA2 resulted in a rich set of neuroscientific data and tools, aiming to bridge the gaps between modalities and scales, leading to the multi-level analyses of the human brain. Bridging the gaps is an enormous challenge, considering the large number of neurons and size of the brain, but mandatory to understand the relationship between brain structure and function. The Neuroinformatics Platform with the atlases contain information regarding the normal structure and operation of the brain (subcellular to global brain function), the diseased brain and the different models of brain circuits. It is increasingly relevant for HBP researchers and the scientific community in general, and for analyzing brain function in both health and disease. It has an impact on the ability to create integrated bottom-up and top-down models of the whole brain. The Human brain Atlas has about 500 visits per day, illustrating the need of the community to get access to such data. Further, the work done in SGA2 lays the groundwork for the integration of the next generation of brain-inspired computing systems.

Besides the difficulties encountered during this phase (e.g., data curation was more time-intensive than expected, a delay in the acquisition of the hippocampal tissue lead to a delay in genetic and receptor analysis of the sample), the main goal of SP2 has been achieved: we provide a new kind of Brain Atlas that allows to access data from all levels of human organization and to link and analyse them through the new platform EBRAINS.